Radiative-Recoil Corrections in Muonium and Positronium

Greg Adkins
Franklin & Marshall College
Lancaster, Pennsylvania, USA
13 June 2024

Radiative-Recoil Corrections in Muonium and Positronium

Motivation
Experimental Situation
Method of Calculation
Progress Report
Conclusion

<u>Student Assistants:</u>
Raisa Richi
Lecheng Ni
Elias Mitchell
Addison Kovats-Bernat

<u>Acknowledgments</u>
NSF PHY-2308792
NIST 60NANB23D230
Franklin & Marshall College

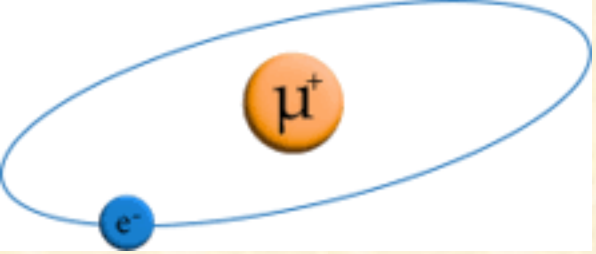

PSAS’2024

Muonium: a purely leptonic exotic atom

Muonium, the μ^+e^- bound system, is closely analogous to hydrogen but with several important differences. First, both of it’s constituents are structureless point-like particles. Compared to hydrogen, where the proton size and internal structure matter, the theoretical analysis of muonium is relatively straightforward. Recoil effects are more important in muonium than in hydrogen, given that $m_e/m_\mu=1/207$ while $m_e/m_p=1/1837$. The finite muon lifetime of $\tau=2.2\ \mu s$ leads to a natural minimum linewidth through the uncertainty principle.

High precision measurements of many of the muonium n=1 and n=2 transitions combined with the possibility of high precision calculation of those transition frequencies based mainly on QED make muonium an attractive system for the determination of fundamental constants and testing the limits of current theory.

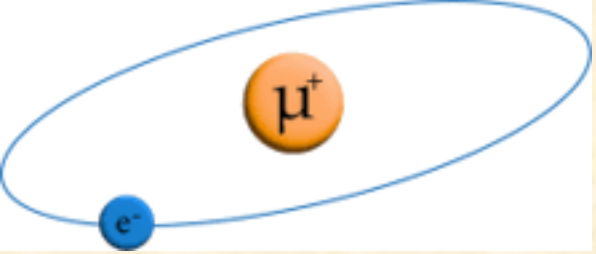

PSAS'2024

Muonium Spectrum

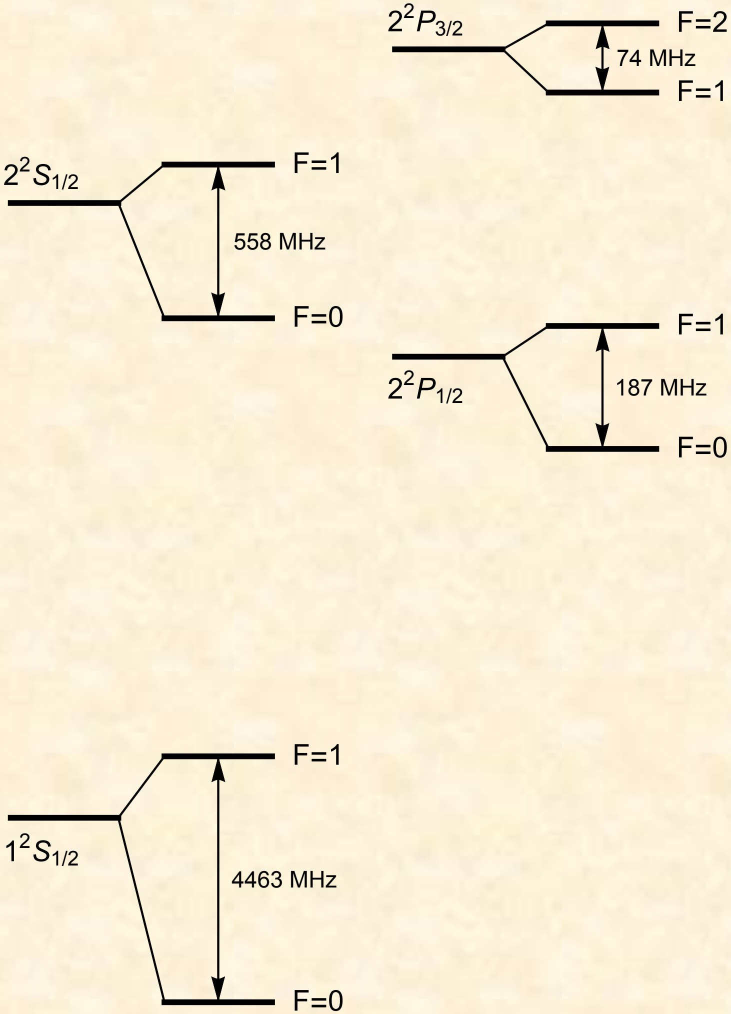

The n=1 and n=2 muonium energy levels are shown, along with the hyperfine intervals.

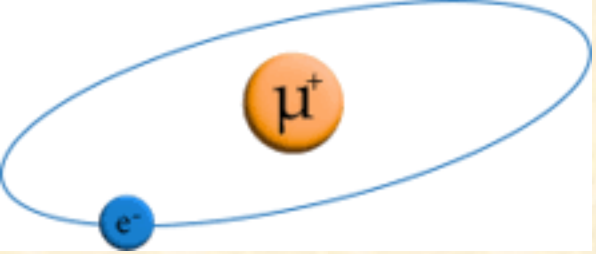

PSAS'2024

Muonium Spectrum

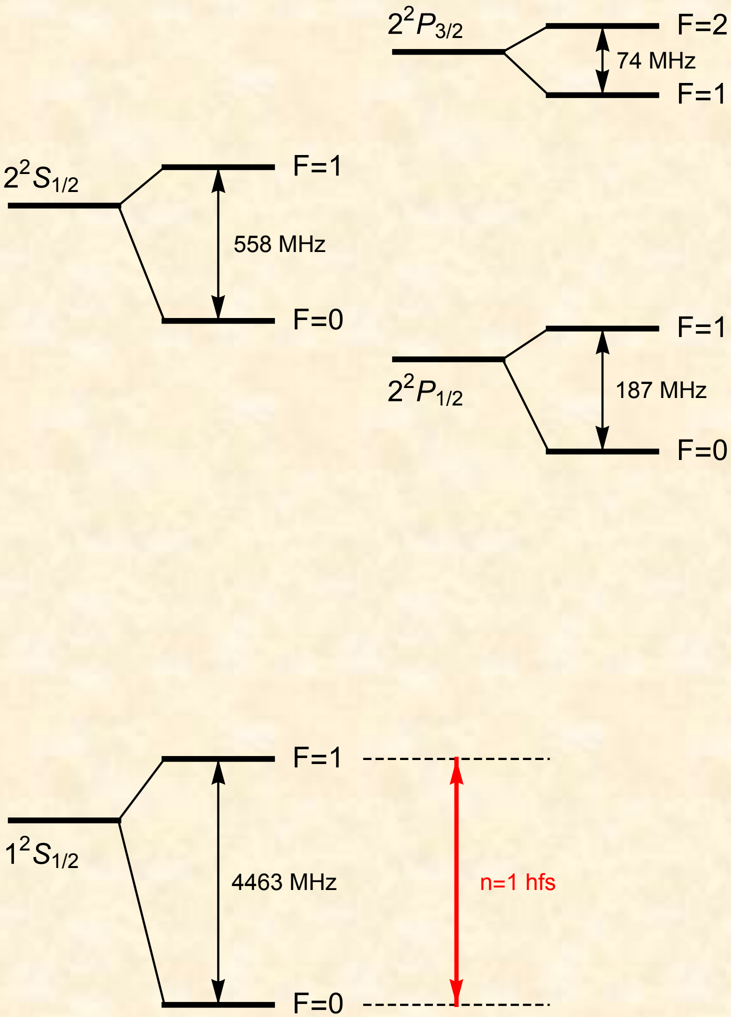

The n=1 hyperfine interval has been measured to high precision:

$$\Delta E = 4\,463\,302.88(16)\,\mathrm{kHz}$$

F.G.Marion et al., Phys. Rev. Lett. 49, 993 (1982)

$$\Delta E = 4\,463\,302.765(53)\,\mathrm{kHz}$$

W.Liu et al., Phys. Rev. Lett. 82, 711 (1999)

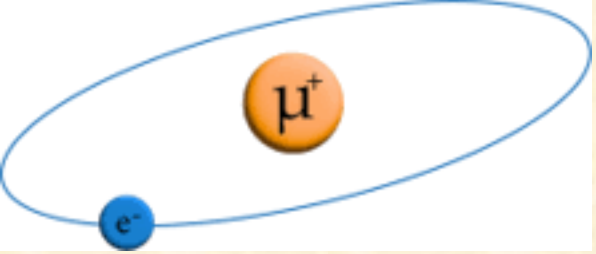

Muonium Spectrum

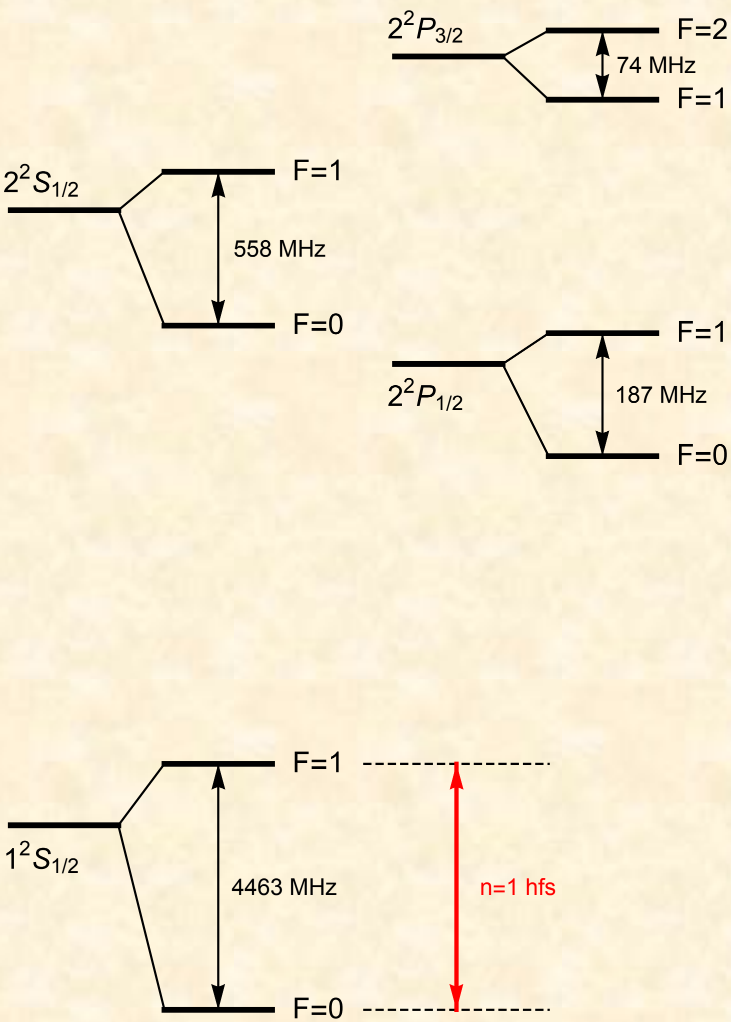

The n=1 hyperfine interval has been measured to high precision:

$$\Delta E = 4\,463\,302.88(16)\,\mathrm{kHz}$$

F.G.Marion et al., Phys. Rev. Lett. 49, 993 (1982)

$$\Delta E = 4\,463\,302.765(53)\,\mathrm{kHz}$$

W.Liu et al., Phys. Rev. Lett. 82, 711 (1999)

$$\Delta E = 4\,463\,302(4)\,\mathrm{kHz}$$

S.Kanda et al. (MuSEUM), Phys. Lett. B 815, 136154 (2021)

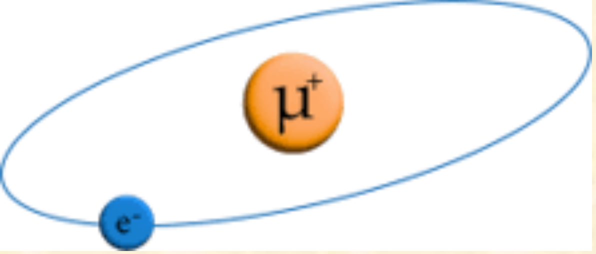

PSAS'2024

Muonium Spectrum

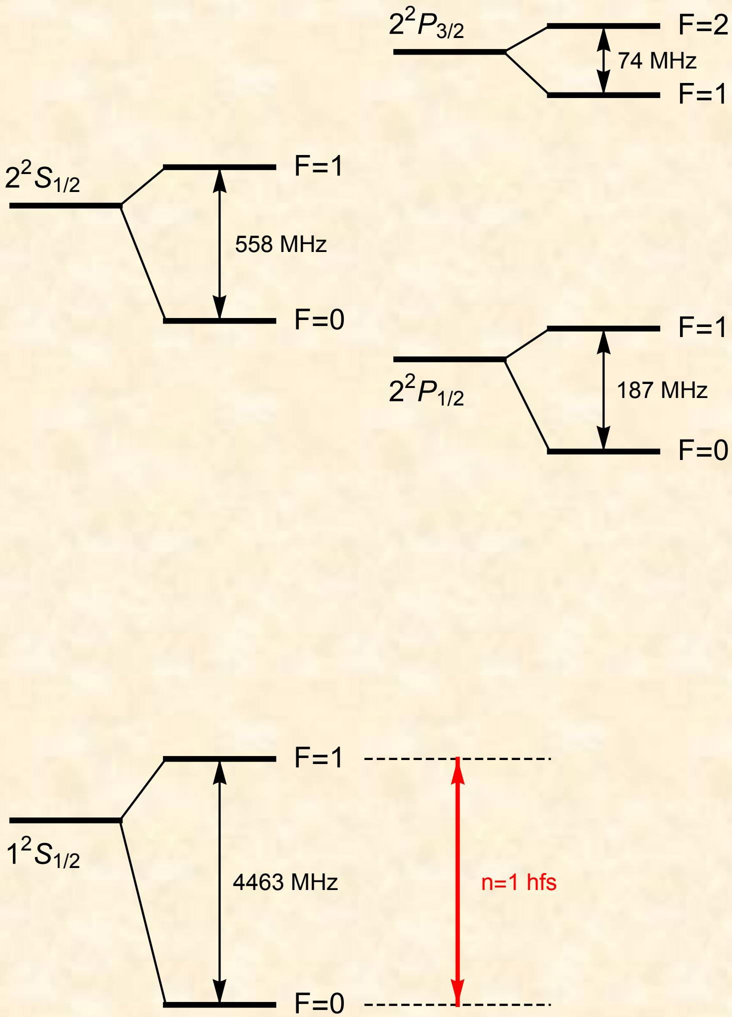

The n=1 hyperfine interval has been measured to high precision:

$$\Delta E = 4\,463\,302.88(16)\,\mathrm{kHz}$$

F.G.Marion et al., Phys. Rev. Lett. 49, 993 (1982)

$$\Delta E = 4\,463\,302.765(53)\,\mathrm{kHz}$$

W.Liu et al., Phys. Rev. Lett. 82, 711 (1999)

$$\Delta E = 4\,463\,302(4)\,\mathrm{kHz}$$

S.Kanda et al. (MuSEUM), Phys. Lett. B 815, 136154 (2021)

The new work has an uncertainty goal of ±5 Hz
P.Strasser et. al. (MuSEUM) EPJ Web of Conferences 198, 00003 (2019)

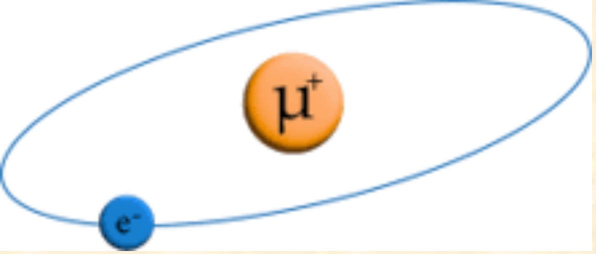

PSAS'2024

Muonium Spectrum

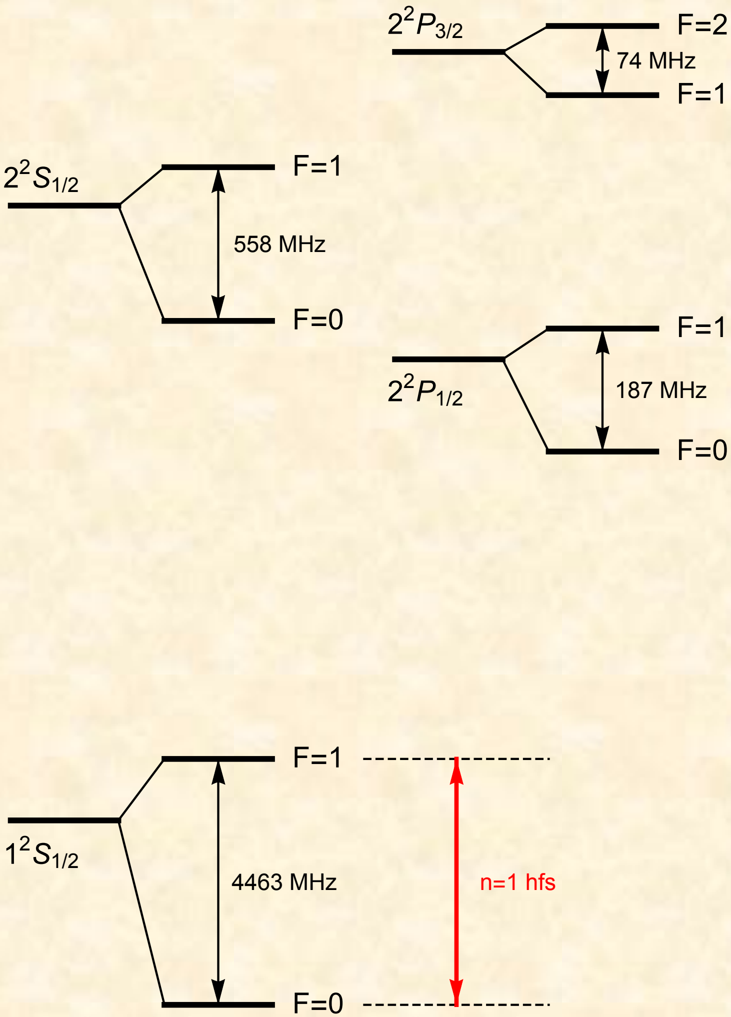

The n=1 hyperfine interval has been measured to high precision:

$$\Delta E = 4\,463\,302.88(16)\,\mathrm{kHz} \qquad \text{(Marion 1982)}$$

$$\Delta E = 4\,463\,302.765(53)\,\mathrm{kHz} \qquad \text{(Liu 1999)}$$

$$\Delta E = 4\,463\,302(4)\,\mathrm{kHz} \qquad \text{(Kanda 2021)}$$

The new experimental work has an uncertainty goal of ±5 Hz.

Theoretical prediction:

$$\Delta E = 4\,463\,302.868(271)\,\mathrm{kHz}$$

Mohr, Newell, Taylor, Rev. Mod. Phys. 88, 035009 (2016)

$$\Delta E = 4\,463\,302.872(515)\,\mathrm{kHz}$$

Eides, Phys. Lett. B 795, 113 (2019)

See also Karshenboim and Korzinin, Phys. Rev. A 103, 022805 (2021)

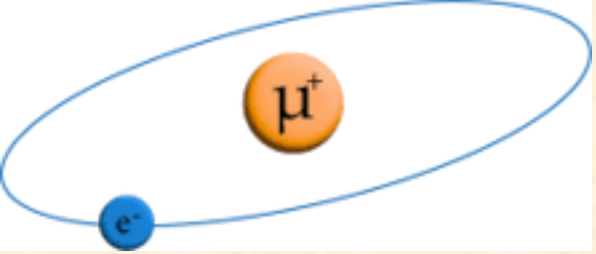

PSAS'2024

Muonium Spectrum

$$\tilde{E}_F = \frac{8m_e\alpha^4}{3}\left(\frac{m_r}{m_e}\right)^3\left(\frac{m_e}{m_\mu}\right) = 4454\,\mathrm{MHz}$$

$$\begin{aligned}\alpha^2\tilde{E}_F\left(\frac{m_e}{m_\mu}\right) &= 1147\,\mathrm{Hz}\,,\\ \alpha^2\tilde{E}_F\left(\frac{m_e}{m_\mu}\right)^2 &= 5.5\,\mathrm{Hz}\,,\\ \alpha^3\tilde{E}_F\left(\frac{m_e}{m_\mu}\right) &= 8.4\,\mathrm{Hz}\end{aligned}$$

$$\ln\left(\frac{1}{\alpha}\right) = 4.92\ \ ,\ \ \ln\left(\frac{m_\mu}{m_e}\right) = 5.33$$

The n=1 hyperfine interval has been measured to high precision:

$$\Delta E = 4\,463\,302.88(16)\,\mathrm{kHz}$$
$$\Delta E = 4\,463\,302.765(53)\,\mathrm{kHz}$$
$$\Delta E = 4\,463\,302(4)\,\mathrm{kHz}$$

The new experimental work has an uncertainty goal of ±5 Hz.

Theoretical prediction:
$\Delta E = 4\,463\,302.868(271)\,\mathrm{kHz}$
Mohr, Newell, Taylor, Rev. Mod. Phys. 88, 035009 (2016). [th: ±85 Hz]
$\Delta E = 4\,463\,302.872(515)\,\mathrm{kHz}$ [th: ±70 Hz]
Eides, Phys. Lett. B 795, 113 (2019)

See also Karshenboim and Korzinin, Phys. Rev. A 103, 022805 (2021)

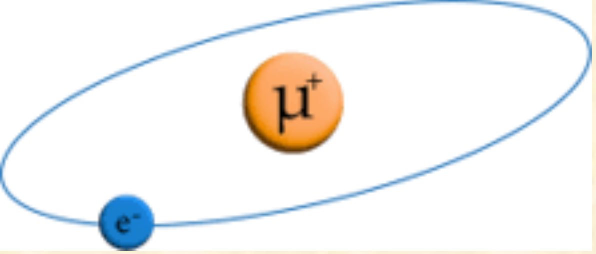

Muonium Spectrum

PSAS'2024

$$\tilde{E}_F = \frac{8 m_e \alpha^4}{3} \left(\frac{m_r}{m_e}\right)^3 \left(\frac{m_e}{m_\mu}\right) = 4454\,\mathrm{MHz}$$

$$\alpha^2 \tilde{E}_F \left(\frac{m_e}{m_\mu}\right) = 1147\,\mathrm{Hz}\,,$$

$$\alpha^2 \tilde{E}_F \left(\frac{m_e}{m_\mu}\right)^2 = 5.5\,\mathrm{Hz}\,,$$

$$\alpha^3 \tilde{E}_F \left(\frac{m_e}{m_\mu}\right) = \boxed{8.4\,\mathrm{Hz}}$$

$$\ln\left(\frac{1}{\alpha}\right) = 4.92 \quad , \quad \ln\left(\frac{m_\mu}{m_e}\right) = 5.33$$

The n=1 hyperfine interval has been measured to high precision:

$$\Delta E = 4\,463\,302.88(16)\,\mathrm{kHz}$$

$$\Delta E = 4\,463\,302.765(53)\,\mathrm{kHz}$$

$$\Delta E = 4\,463\,302(4)\,\mathrm{kHz}$$

The new experimental work has an uncertainty goal of ±5 Hz.

Theoretical prediction:

$\Delta E = 4\,463\,302.868(271)\,\mathrm{kHz}$

Mohr, Newell, Taylor, Rev. Mod. Phys. 88, 035009 (2016). [th: ±85 Hz]

$\Delta E = 4\,463\,302.872(515)\,\mathrm{kHz}$ [th: ±70 Hz]

Eides, Phys. Lett. B 795, 113 (2019)

See also Karshenboim and Korzinin, Phys. Rev. A 103, 022805 (2021)

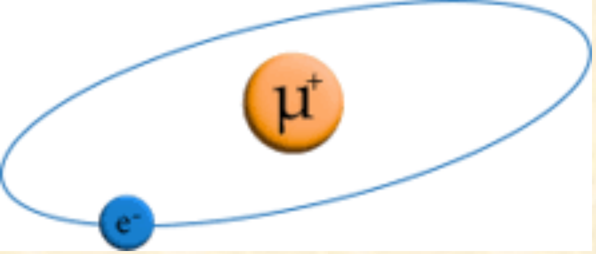

PSAS'2024

Muonium Spectrum: 1S-2S Interval

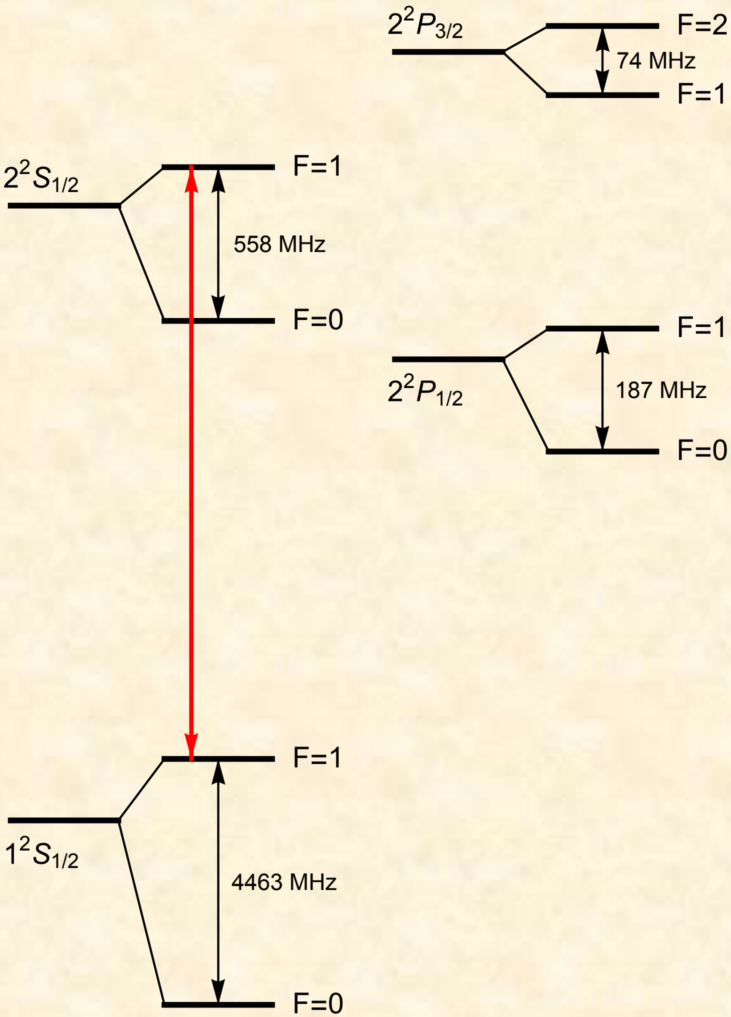

The 1S-2S interval has a natural linewidth of 145 kHz and can be measured with great precision.

V. Meyer et al., Phys. Rev. Lett. 84, 1136 (2000)

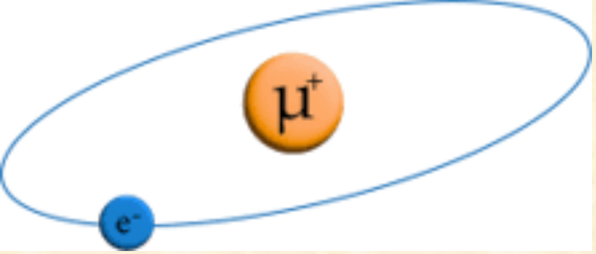

PSAS'2024

Muonium Spectrum: 1S-2S Interval

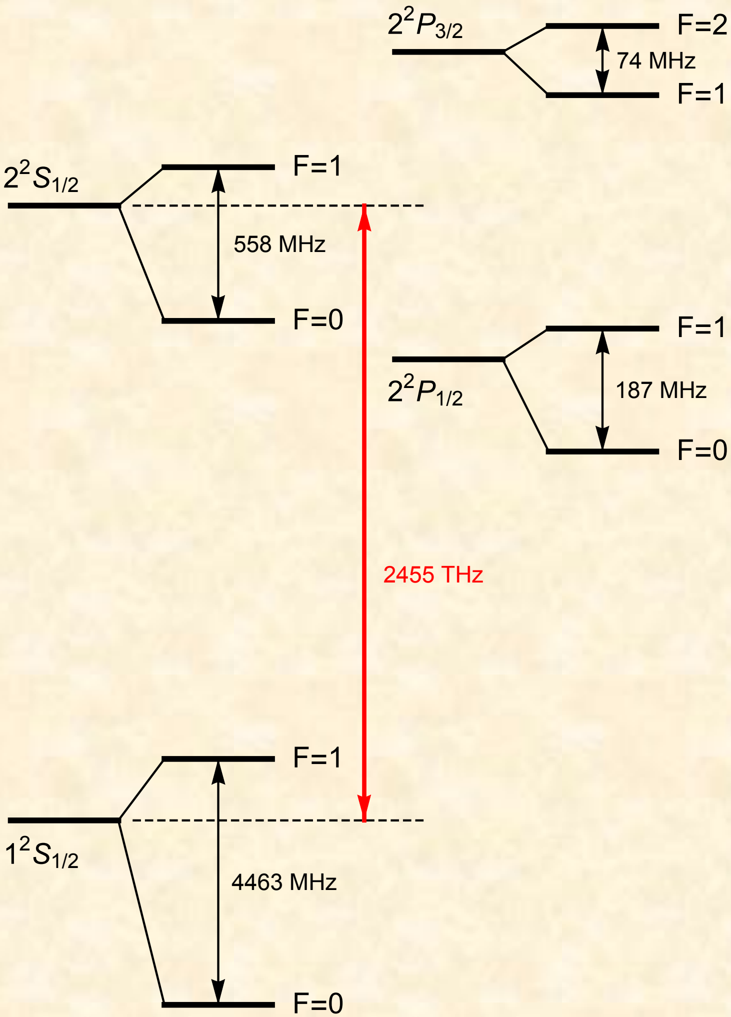

The 1S-2S interval has a natural linewidth of 145 kHz and can be measured with great precision:

$\Delta\nu$=2,455,528,941.0(9.8) MHz (4 ppb)

V. Meyer et al., Phys. Rev. Lett. 84, 1136 (2000).

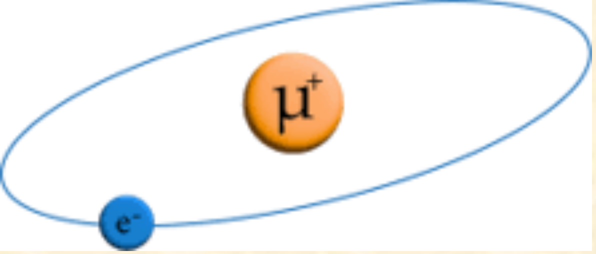

PSAS'2024

Muonium Spectrum: 1S-2S Interval

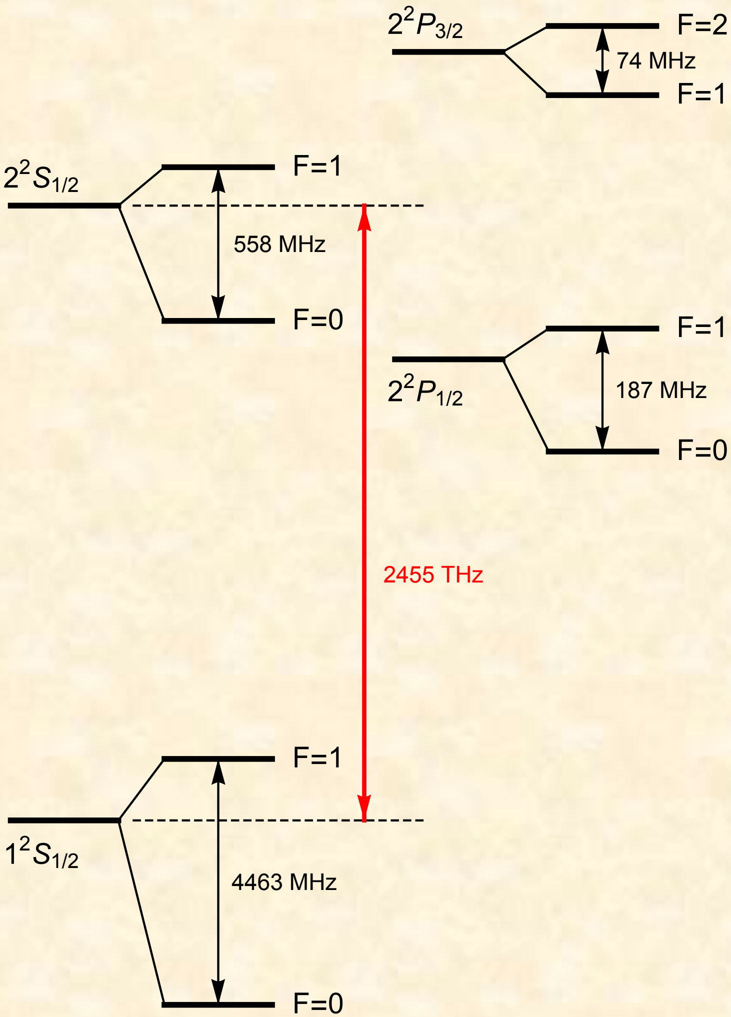

The 1S-2S interval has a natural linewidth of 145 kHz and can be measured with great precision:
$\Delta\nu$=2,455,528,941.0(9.8) MHz (4 ppb)
V. Meyer et al., Phys. Rev. Lett. 84, 1136 (2000).

The theoretical prediction is:
$\Delta\nu$=2,455,528,935.4(1.4) MHz
K. Pachucki et al., J. Phys. B 29, 177 (1996). The QED part of the uncertainty is ±6 kHz.

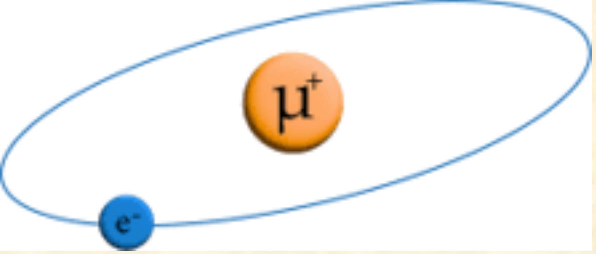

Muonium Spectrum: 1S-2S Interval

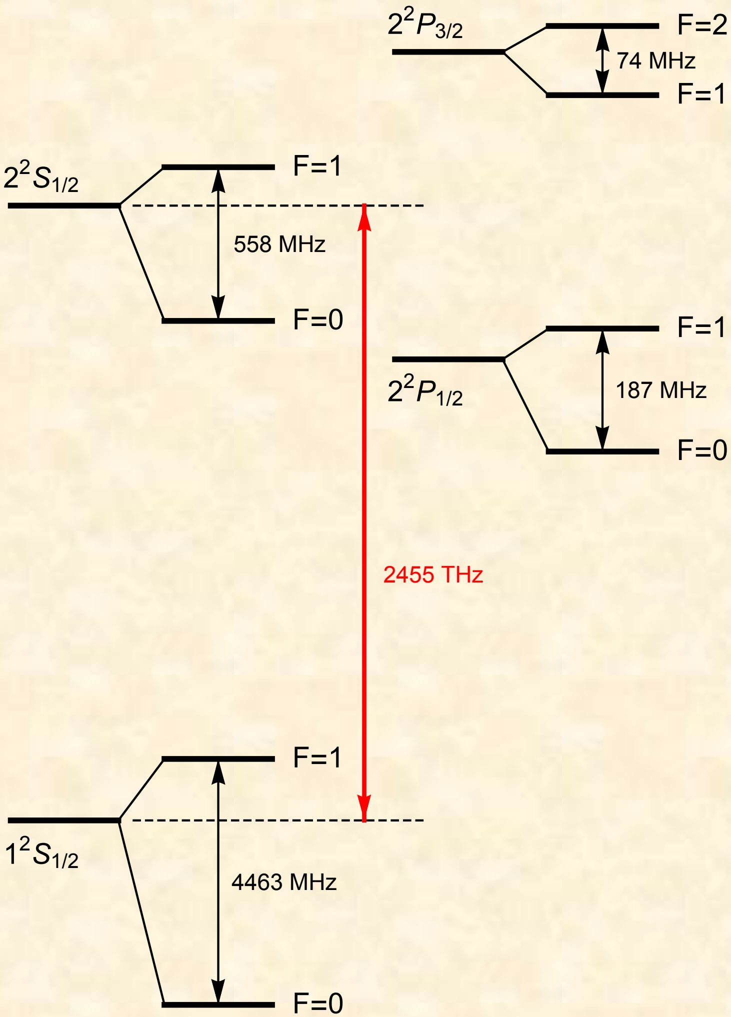

The 1S-2S interval has a natural linewidth of 145 kHz and can be measured with great precision:
Δν=2,455,528,941.0(9.8) MHz (4 ppb)
V. Meyer et al., Phys. Rev. Lett. 84, 1136 (2000).

The theoretical prediction is:
Δν=2,455,528,935.4(1.4) MHz
K. Pachucki et al., J. Phys. B 29, 177 (1996). The QED part of the uncertainty is ±6 kHz.

The present Mu-MASS goal is for an uncertainty of ±10 kHz (4 ppt)
I. Cortinovis et al., Eur. Phys. J. D 77, 66 (2023).

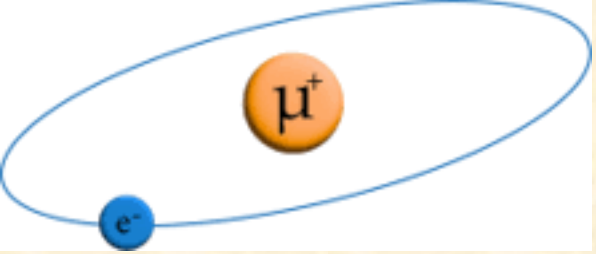

Muonium Spectrum: 1S-2S Interval

$$m_e\alpha^6\left(\frac{m_r}{m_e}\right)^3\left(\frac{m_e}{m_\mu}\right) = 88.9\,\mathrm{kHz}\,,$$
$$m_e\alpha^6\left(\frac{m_r}{m_e}\right)^3\left(\frac{m_e}{m_\mu}\right)^2 = 0.43\,\mathrm{kHz}\,,$$
$$m_e\alpha^7\left(\frac{m_r}{m_e}\right)^3\left(\frac{m_e}{m_\mu}\right) = 0.65\,\mathrm{kHz}$$

$$\ln\left(\frac{1}{\alpha}\right) = 4.92\ , \quad \ln\left(\frac{m_\mu}{m_e}\right) = 5.33$$

The 1S-2S interval has a natural linewidth of 145 kHz and can be measured with great precision:
Δν=2,455,528,941.0(9.8) MHz (4 ppb)
V. Meyer et al., Phys. Rev. Lett. 84, 1136 (2000).

The theoretical prediction is:
Δν=2,455,528,935.4(1.4) MHz
K. Pachucki et al., J. Phys. B 29, 177 (1996). The QED part of the uncertainty is ±6 kHz.

The present Mu-MASS goal is for an uncertainty of ±10 kHz (4 ppt)
I. Cortinovis et al., Eur. Phys. J. D 77, 66 (2023).

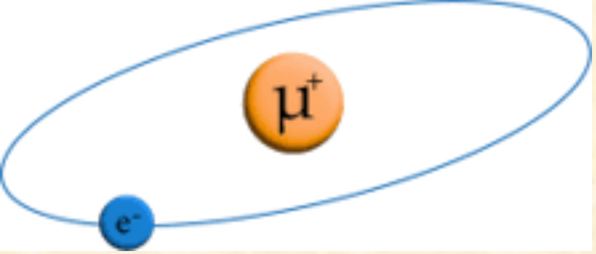

PSAS'2024

Muonium Spectrum: Lamb Shift

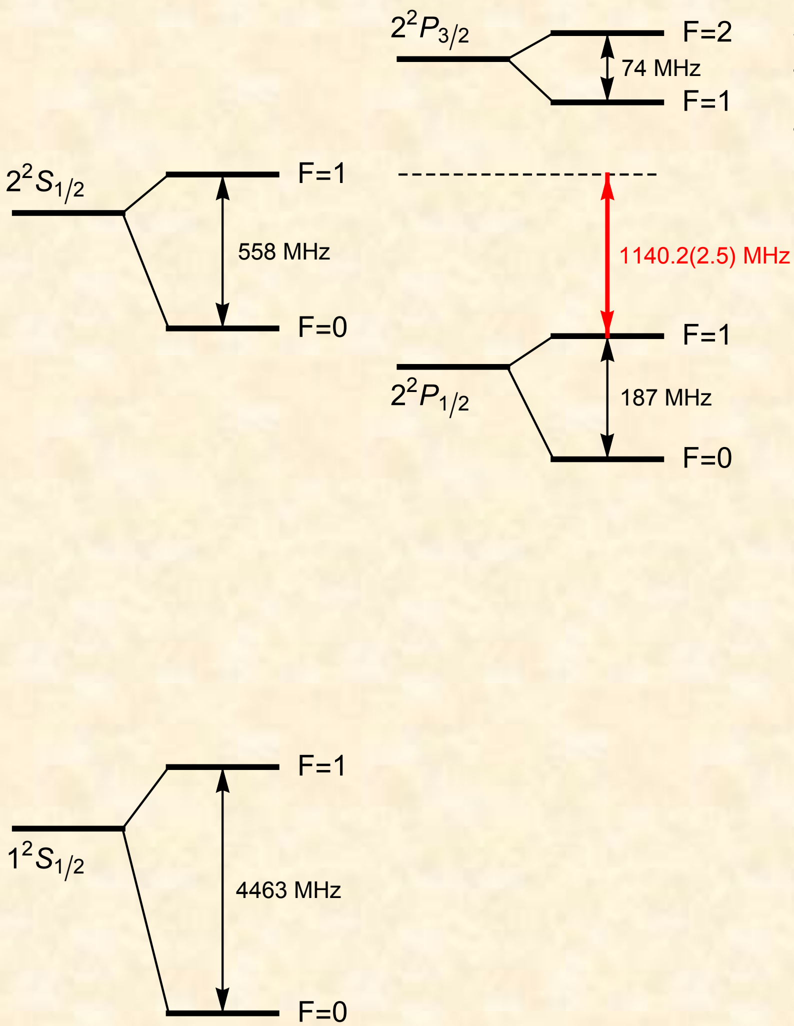

A recent measurement of one of the n=2 transitions, combined with hfs values, allows the determination of the Lamb Shift.

B. Ohayon et al., Phys. Rev. Lett. 128, 011802 (2022)

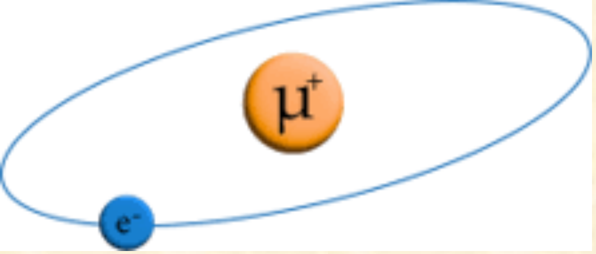

PSAS'2024

Muonium Spectrum: Lamb Shift

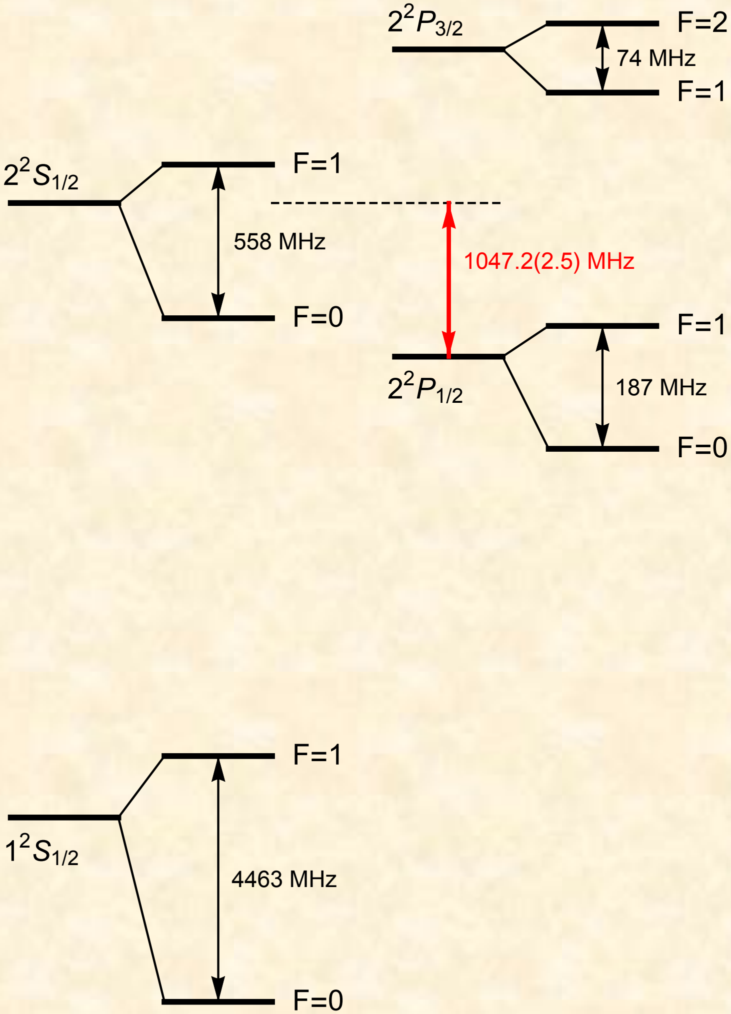

A recent measurement of one of the n=2 transitions, combined with hfs values, allows the determination of the Lamb Shift.

$$\Delta E = 1047.2(2.5)\ \mathrm{MHz}$$

B. Ohayon et al., Phys. Rev. Lett. 128, 011802 (2022)

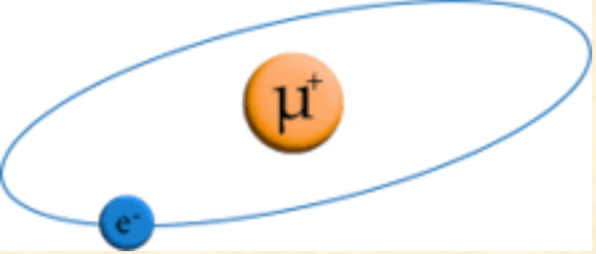

PSAS'2024

Muonium Spectrum: Lamb Shift

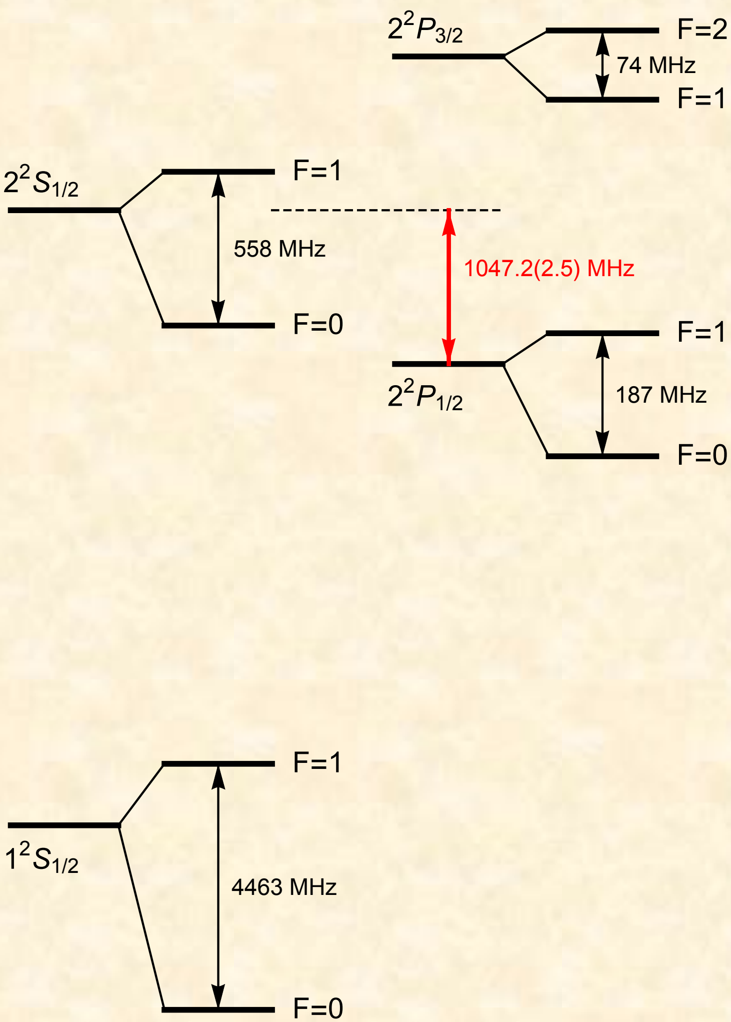

A recent measurement of one of the n=2 transitions, combined with hfs values, allows the determination of the Lamb Shift.

$$\Delta E = 1047.2(2.5)\,\mathrm{MHz}$$

B. Ohayon et al., Phys. Rev. Lett. 128, 011802 (2022)

Possible improvements to ±0.300 MHz, or perhaps ±0.030 MHz.

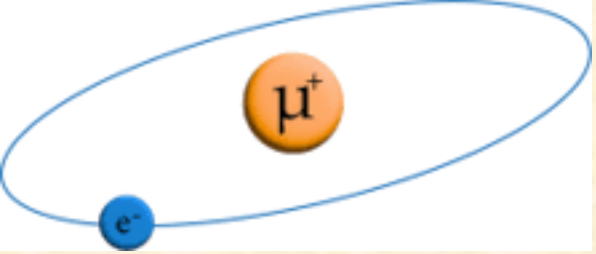

PSAS'2024

Muonium Spectrum: Lamb Shift

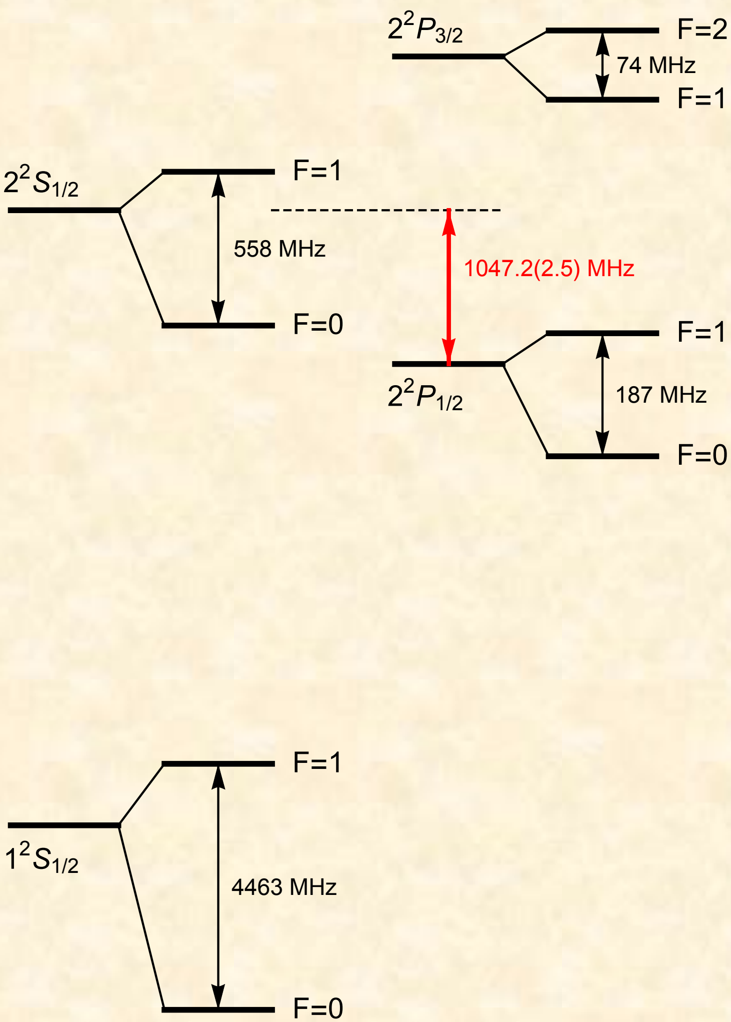

A recent measurement of one of the n=2 transitions, combined with hfs values, allows the determination of the Lamb Shift.

$$\Delta E = 1047.2(2.5)\,\mathrm{MHz}$$

B. Ohayon et al., Phys. Rev. Lett. 128, 011802 (2022)

Possible improvements to ±0.300 MHz, or perhaps ±0.030 MHz.

Theoretical predictions:

$$\Delta E = 1047.498(1)\,\mathrm{MHz}$$

Janka, Ohayon, Crivelli, EPJ Conf. 262, 01001 (2022)

$$\Delta E = 1047.284(2)\,\mathrm{MHz}$$

Frugiuele, Pérez-Ríos, Peset, Phys. Rev. D 100, 015010 (2019) [done using pNRQED]

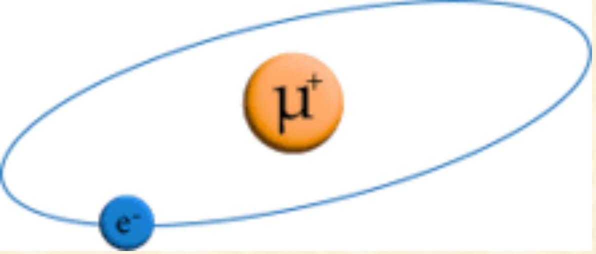

Muonium Spectrum: Lamb Shift

PSAS'2024

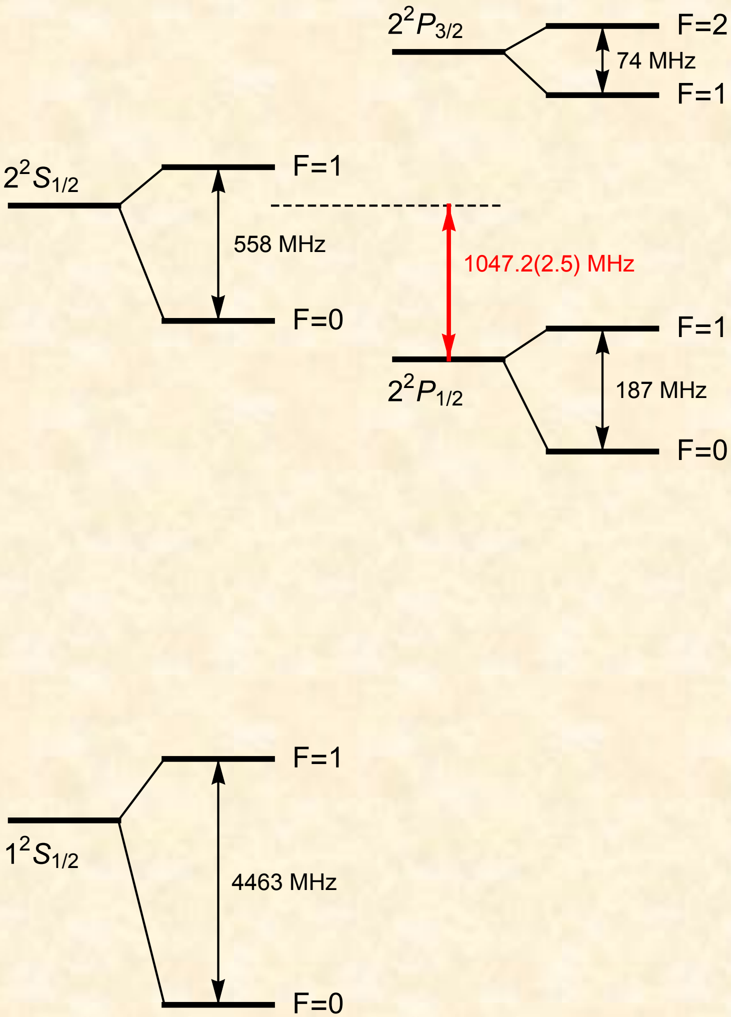

A recent measurement of one of the n=2 transitions, combined with hfs values, allows the determination of the Lamb Shift.

$$\Delta E = 1047.2(2.5)\,\mathrm{MHz}$$

B. Ohayon et al., Phys. Rev. Lett. 128, 011802 (2022)

Possible improvements to ±0.300 MHz, or perhaps ±0.030 MHz.

Theoretical predictions:

$$\boxed{\Delta E = 1047.498(1)\,\mathrm{MHz}}$$

Janka, Ohayon, Crivelli, EPJ Conf. 262, 01001 (2022)

$$\boxed{\Delta E = 1047.284(2)\,\mathrm{MHz}}$$

Frugiuele, Pérez-Ríos, Peset, Phys. Rev. D 100, 015010 (2019) [done using pNRQED]

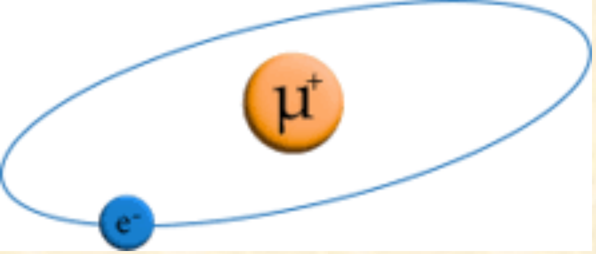

Method of Calculation

1. Use Non-Relativistic QED (NRQED) and dimensional regularization
2. Obtain all required matching coefficients. (Finding the contact term matching coefficients is an essential part of the recoil calculation, and is a significant challenge.)
3. Describe two-body bound states using the NRQED Bethe-Salpeter equation. Energies appear as poles in the Green function
4. Build a perturbation scheme based on an exact lowest-order solution to the NRQED Bethe-Salpeter equation
5. Use "expansion by regions" to identify contributions at various powers of the expansion parameter α
6. Express all contributions in terms of expectation values of various operators in states of the D-dimensional non-relativistic Schrödinger- Coulomb equation. Take the limit $D = 3\text{-}2\epsilon \rightarrow 3$

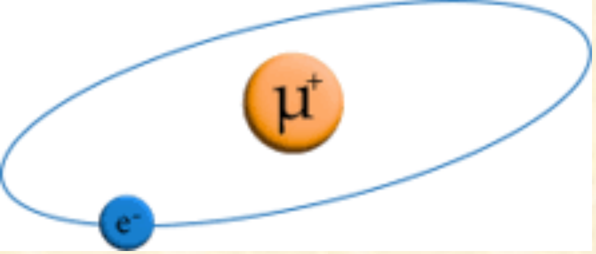

PSAS'2024

NRQED Feynman Rules

Interaction Vertices:

Coulomb

$-\mathrm{iq}$

Spin–Orbit

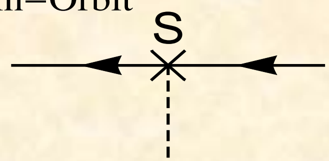

$c_S \dfrac{q}{4\,m^2}(\vec{p}_2 \times \vec{p}_1)\cdot\vec{\sigma}$

Convection

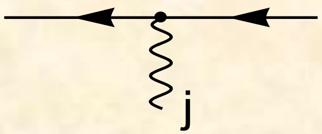

$\dfrac{\mathrm{iq}}{2\,m}(p_2+p_1)_j$

Darwin

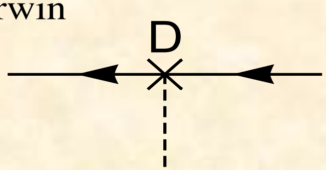

$c_D \dfrac{\mathrm{iq}}{8\,m^2}(\vec{p}_2-\vec{p}_1)^2$

Fermi

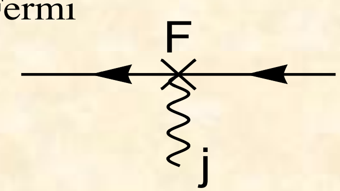

$c_F \dfrac{q}{2\,m}[(\vec{p}_2-\vec{p}_1)\times\vec{\sigma}]_j$

Seagull

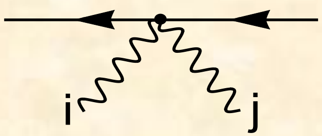

$\dfrac{-\mathrm{iq}^2}{m}\delta_{\mathrm{ij}}$

Contact

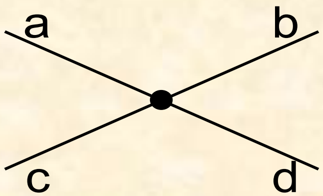

$\dfrac{d_s}{m^2}\delta_{\mathrm{ab}}\delta_{\mathrm{cd}} + \dfrac{d_v}{m^2}\vec{\sigma}_{\mathrm{ab}}\cdot\vec{\sigma}_{\mathrm{cd}}$

$+\cdots$

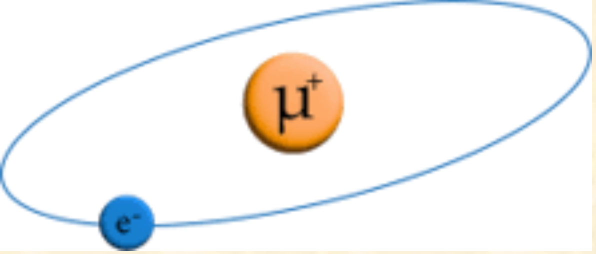

Method of Calculation

1. Use Non-Relativistic QED (NRQED) and dimensional regularization
2. Obtain all required matching coefficients. (Finding the contact term matching coefficients is an essential part of the recoil calculation, and is a significant challenge.)
3. Describe two-body bound states using the NRQED Bethe-Salpeter equation. Energies appear as poles in the Green function
4. Build a perturbation scheme based on an exact lowest-order solution to the NRQED Bethe-Salpeter equation
5. Use "expansion by regions" to identify contributions at various powers of the expansion parameter α
6. Express all contributions in terms of expectation values of various operators in states of the D-dimensional non-relativistic Schrödinger- Coulomb equation. Take the limit $D = 3\text{-}2\epsilon \rightarrow 3$

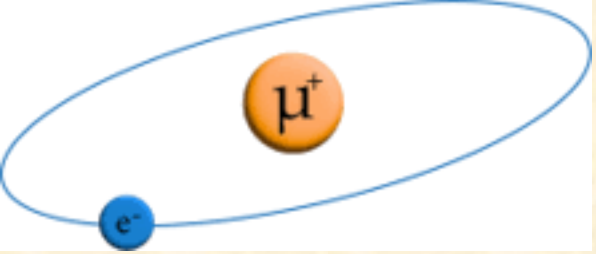

The NRQED Contact Term

The NRQED contact term contains the contributions of all photon-exchange diagrams (possibly including radiative corrections) containing purely relativistic momenta.

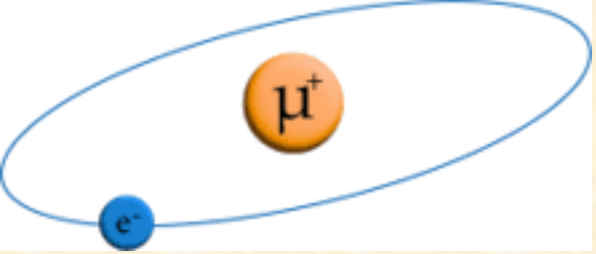

PSAS'2024

The NRQED Contact Term

The idea is that the space-time size of a relativistic process is small on an atomic scale.

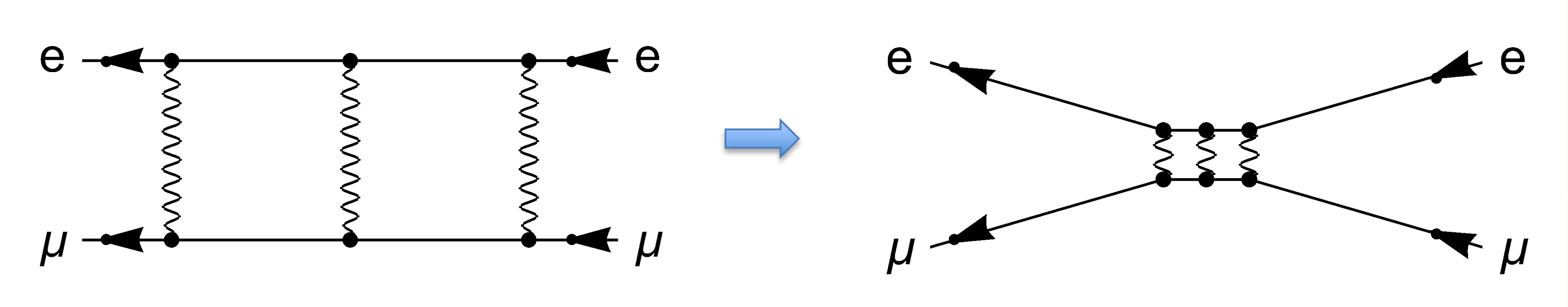

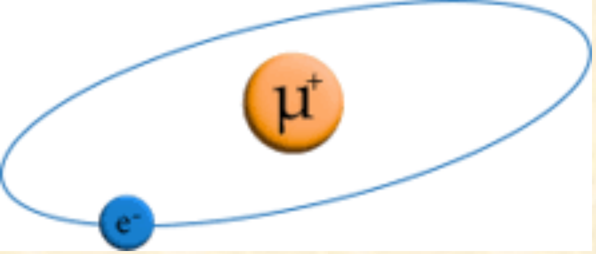

PSAS'2024

The NRQED Contact Term

The idea is that the space-time size of a relativistic process is small on an atomic scale.

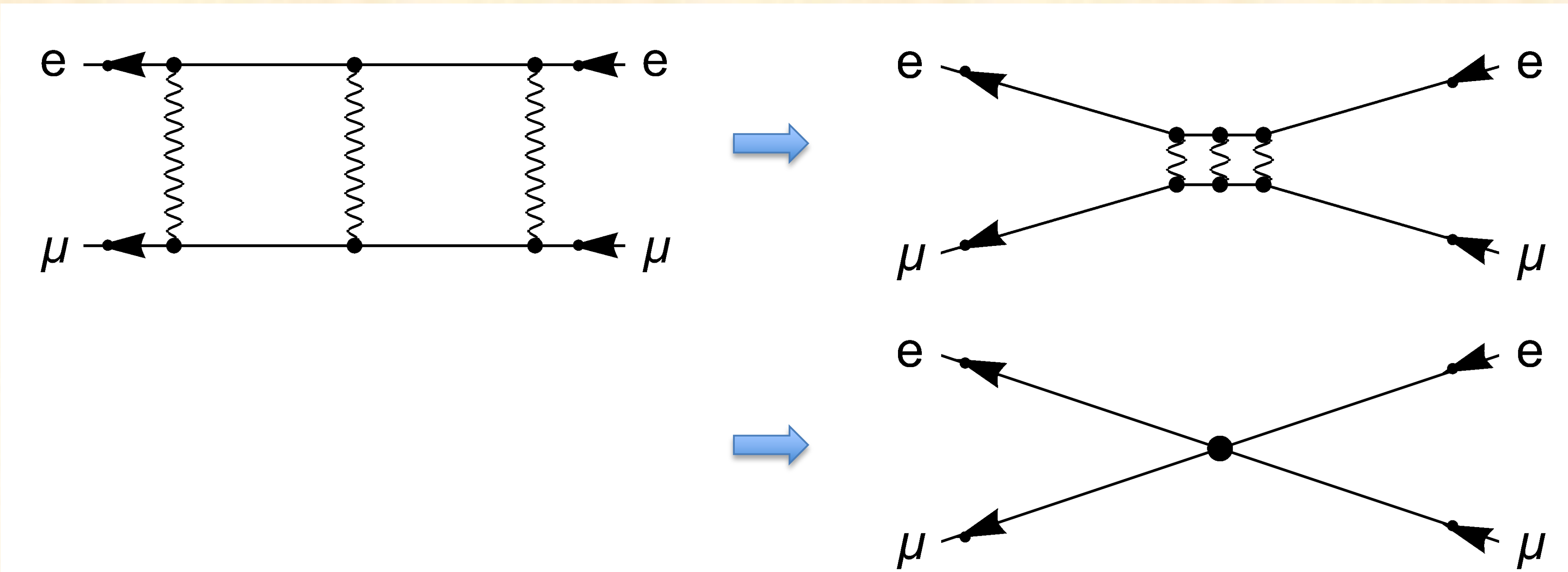

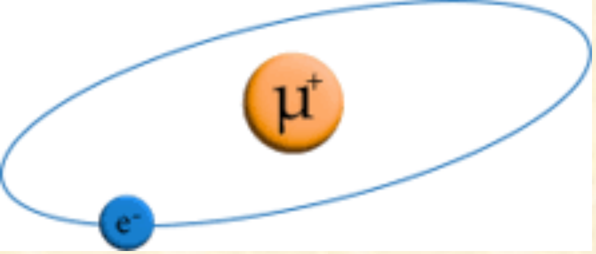

Energy Correction due to the Contact Term

The contact term contributes to an energy shift in NRQED by first order perturbation theory. The contact term matching coefficients are calculated from QED by taking the threshold limit of graphs where all loop momenta are hard (*i.e.* relativistic). Because the contact term has all particles meeting at a point, the energy shift is proportional to the square of the wave function at contact (*i.e.* at zero relative displacement).

$\Delta E \propto$ 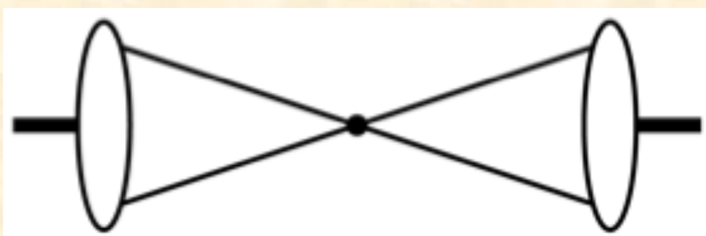 $\propto \ |\psi(0)|^2$ 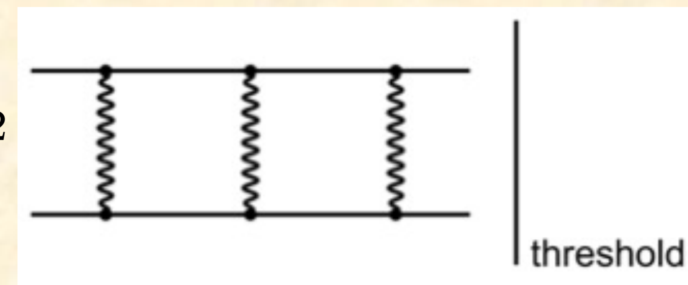

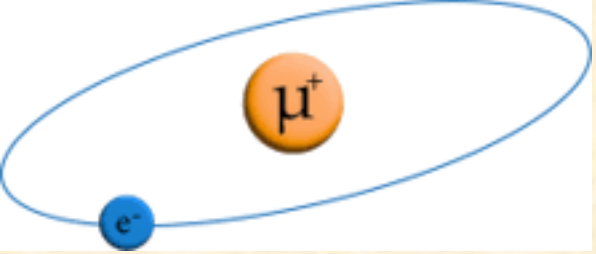

Energy Correction due to the Contact Term

The contact term contributes to an energy shift in NRQED by first order perturbation theory. The contact term matching coefficients are calculated from QED by taking the threshold limit of graphs where all loop momenta are hard (*i.e.* relativistic). Because the contact term has all particles meeting at a point, the energy shift is proportional to the square of the wave function at contact (*i.e.* at zero relative displacement).

$\Delta E \propto$

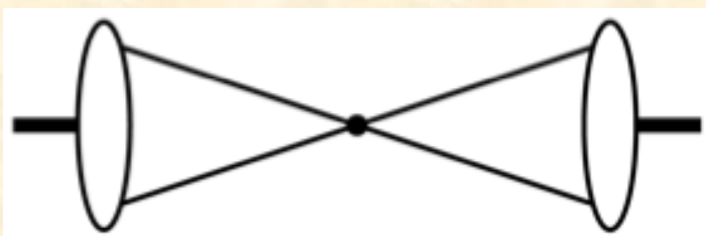

$\propto \; |\psi(0)|^2$

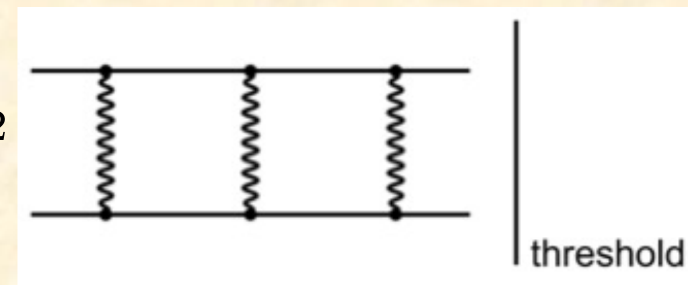

$$\Delta E = -|\psi(0)|^2 \mathcal{M} = -\frac{m_r^3 (Z\alpha)^3}{\pi n^3} \mathcal{M}$$

where $\mathcal{M}$ is the amplitude for hard corrections to QED threshold scattering

Recoil Diagrams at Order $(Z\alpha)^6$

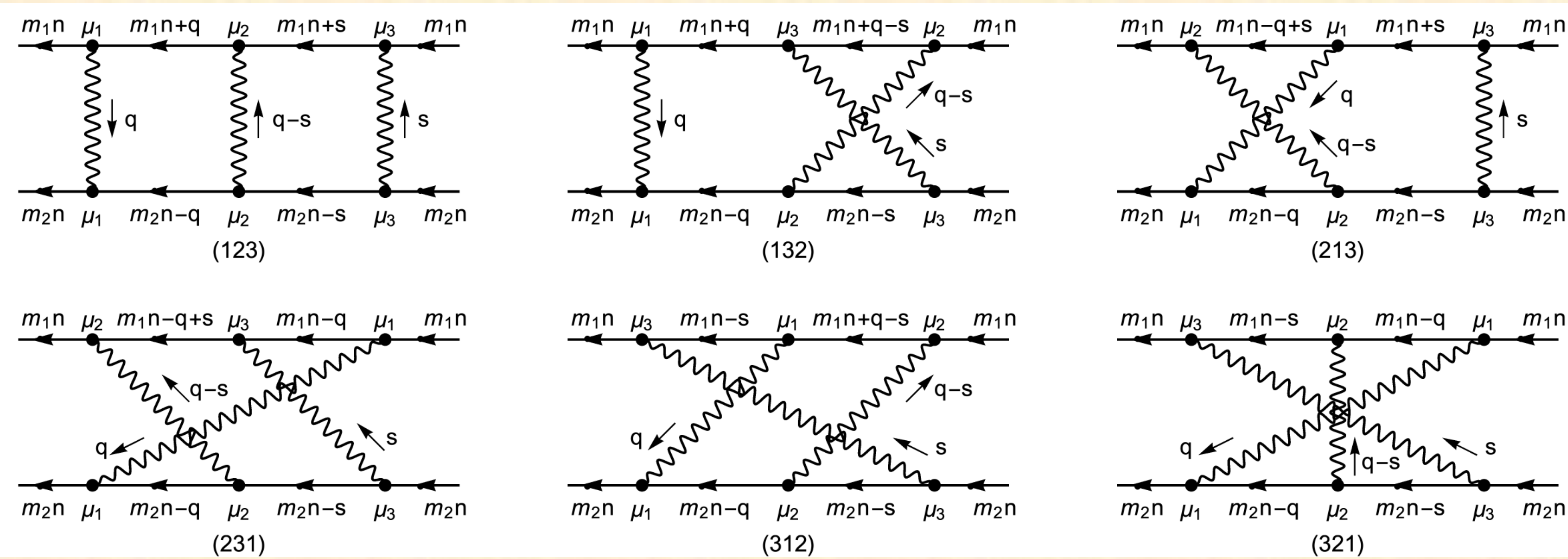

(123) (132) (213)

(231) (312) (321)

Radiative – Recoil Diagrams at Order $\alpha(\mathbf{Z}\alpha)^5$

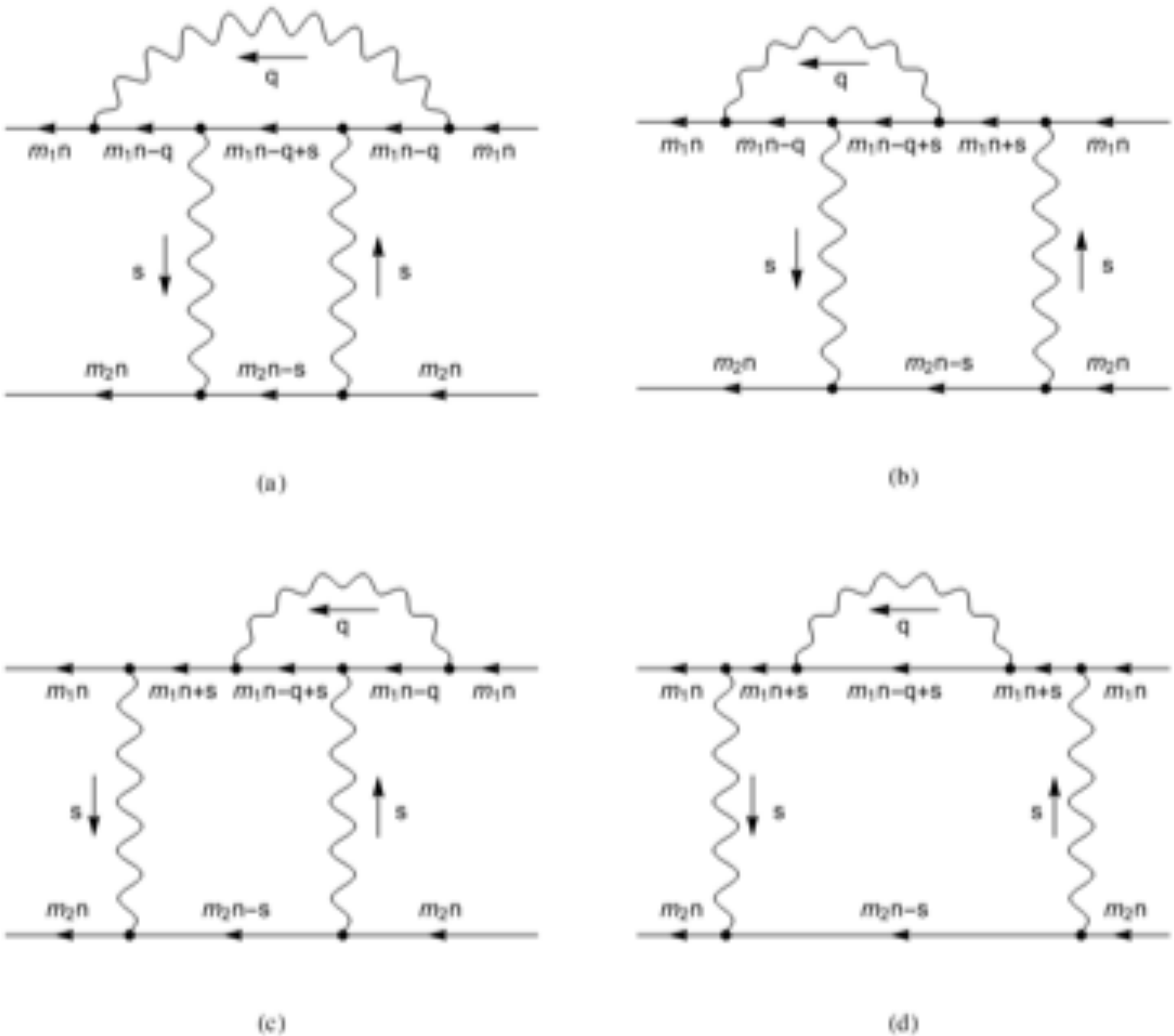

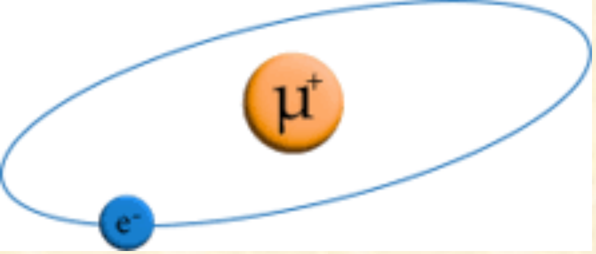

PSAS'2024

Next Steps: Recoil and Radiative-Recoil Corrections at order α^7

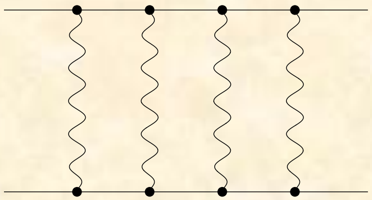

Pure recoil at order $$\frac{m_e(Z\alpha)^7}{n^3}\left(\frac{m_r}{m_e}\right)^3\left(\frac{m_e}{m_\mu}\right)$$

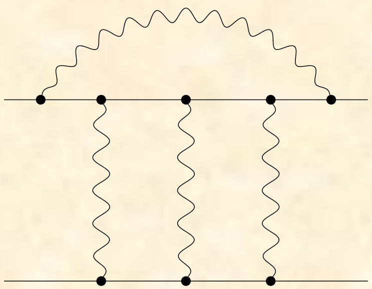

Radiative-recoil at order $$\frac{m_e\alpha(Z\alpha)^6}{n^3}\left(\frac{m_r}{m_e}\right)^3\left(\frac{m_e}{m_\mu}\right)$$

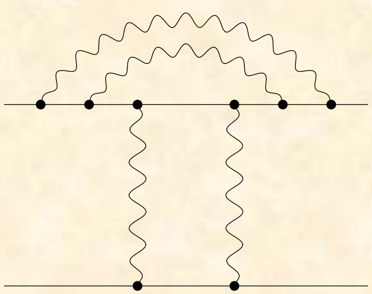

Radiative-recoil at order $$\frac{m_e\alpha^2(Z\alpha)^5}{n^3}\left(\frac{m_r}{m_e}\right)^3\left(\frac{m_e}{m_\mu}\right)$$

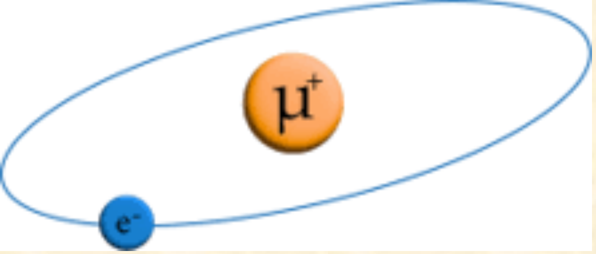

Next Steps: Recoil and Radiative-Recoil Corrections at order α^7

PSAS'2024

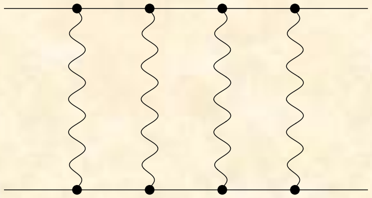

Pure recoil at order $$\frac{m_e(Z\alpha)^7}{n^3}\left(\frac{m_r}{m_e}\right)^3\left(\frac{m_e}{m_\mu}\right)$$

There are 4! = 24 permutations of the photon lines, giving diagrams with crossed photons. Of these, 18 are independent.

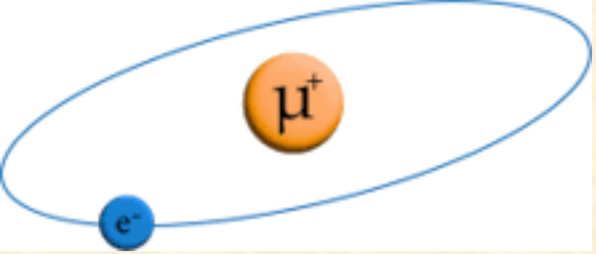

Next Steps: Recoil and Radiative-Recoil Corrections at order α^7

PSAS'2024

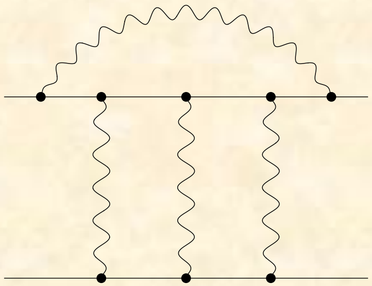

Radiative-recoil at order $$\frac{m_e\alpha(Z\alpha)^6}{n^3}\left(\frac{m_r}{m_e}\right)^3\left(\frac{m_e}{m_\mu}\right)$$

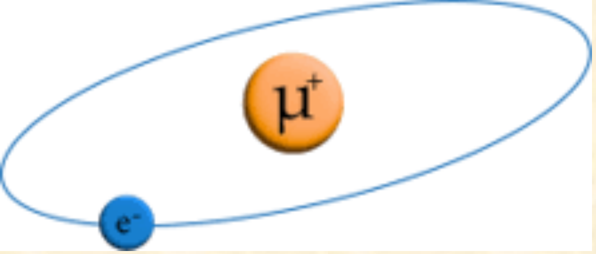

PSAS'2024

Radiative–Recoil Diagrams at Order $\alpha(Z\alpha)^6$

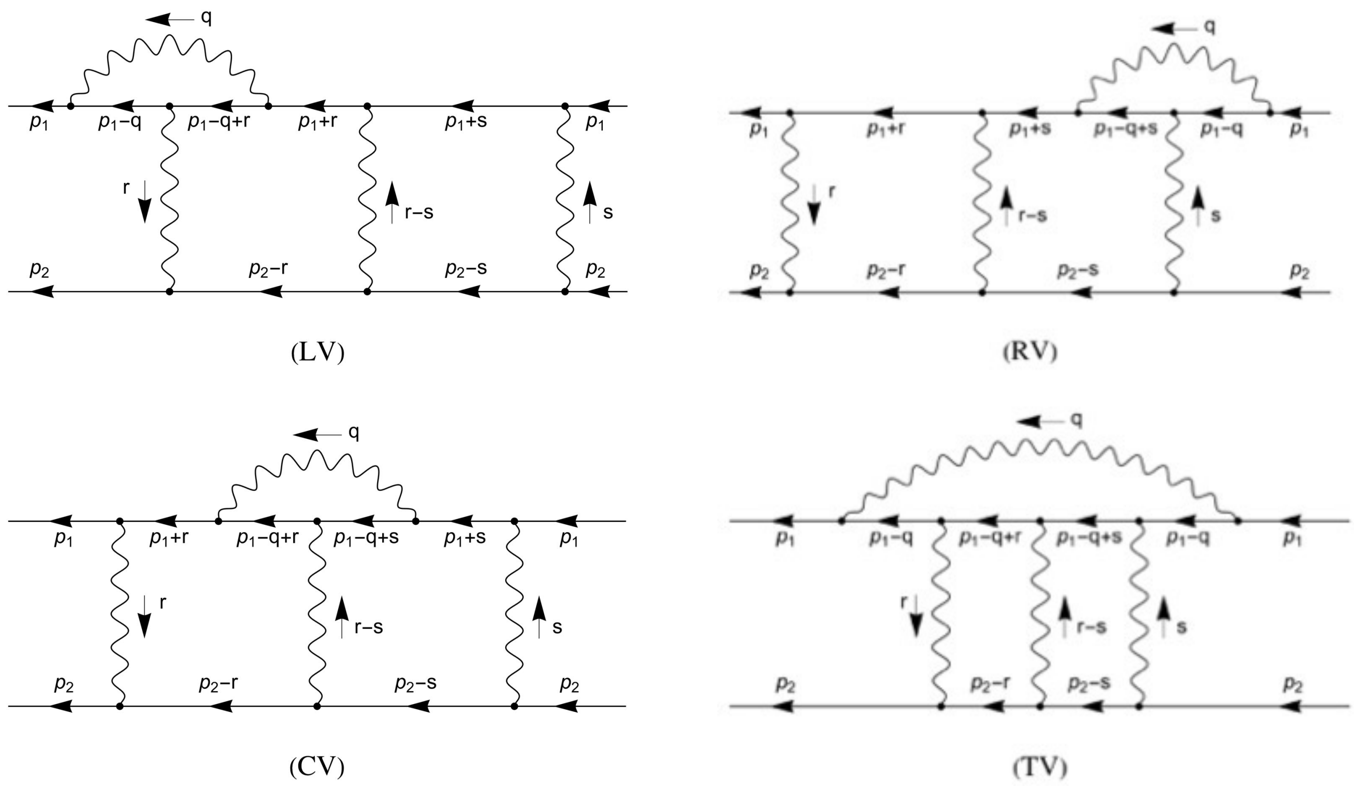

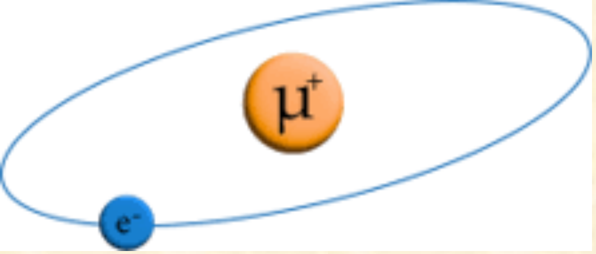

Radiative−Recoil Diagrams
at Order $\alpha(Z\alpha)^6$

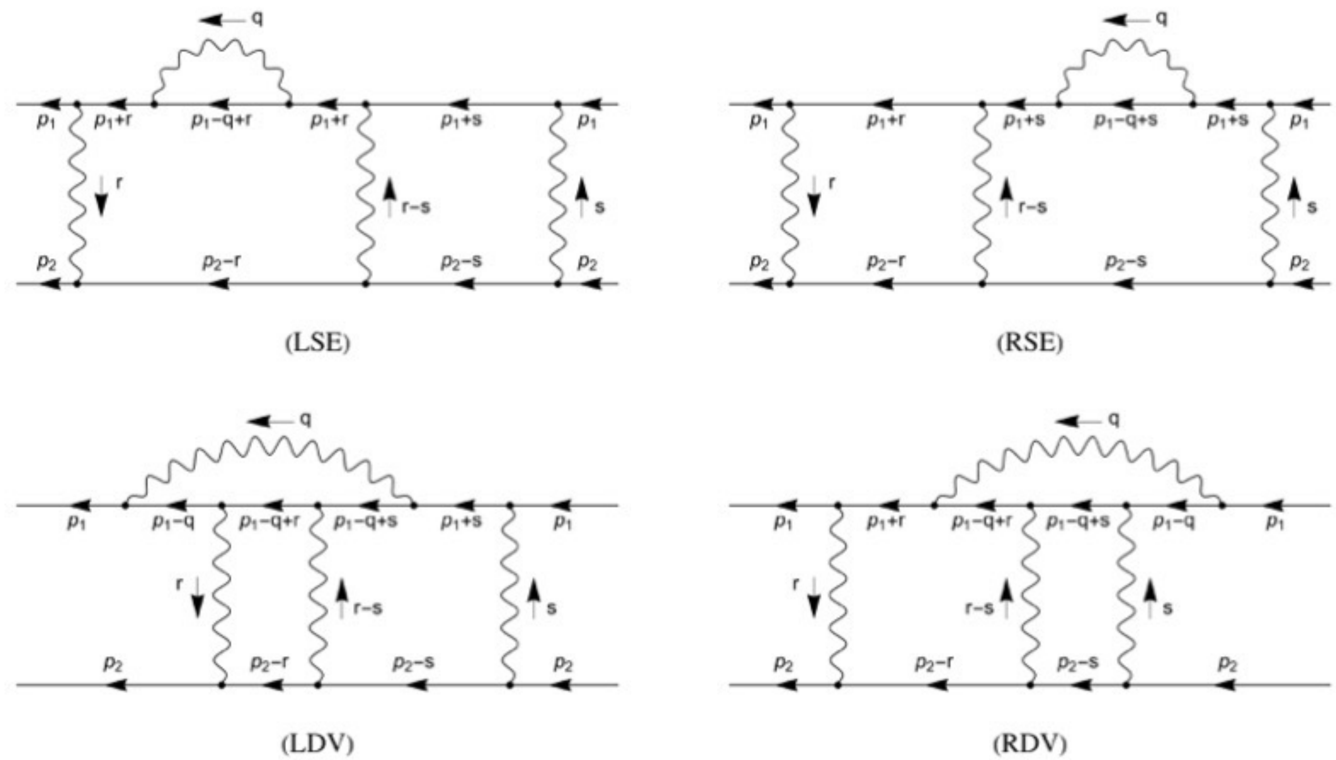

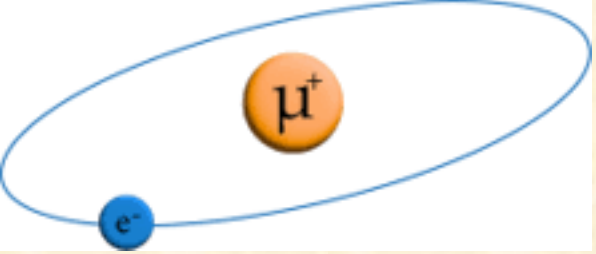

PSAS'2024

Next Steps: Recoil and Radiative-Recoil Corrections at order α^7

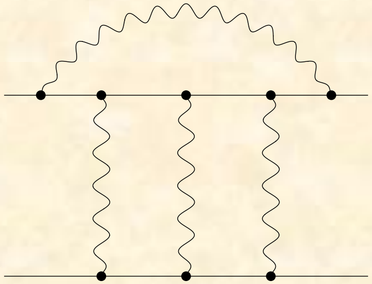

Radiative-recoil at order $\dfrac{m_e\alpha(Z\alpha)^6}{n^3}\left(\dfrac{m_r}{m_e}\right)^3\left(\dfrac{m_e}{m_\mu}\right)$

There are 8 diagrams with ladder photons, and 3! = 6 permutations of those photons giving 6 x 8 = 48 diagrams when all diagrams with crossed photons are included. Of these, 26 are independent.

The IBP relations are being used to express these 26 diagrams in terms of master integrals.

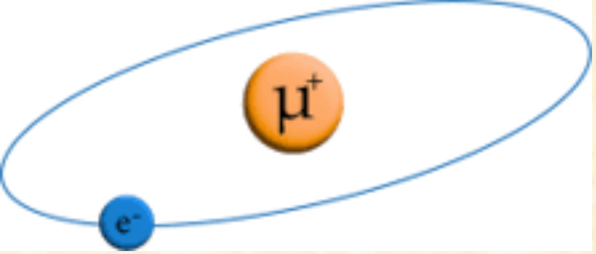

Next Steps: Recoil and Radiative-Recoil Corrections at order α^7

PSAS'2024

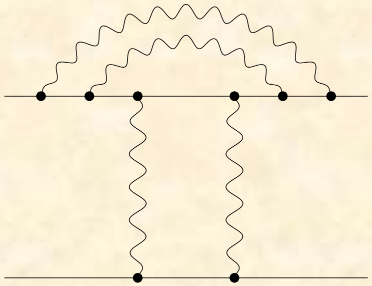

Radiative-recoil at order $$\frac{m_e\alpha^2(Z\alpha)^5}{n^3}\left(\frac{m_r}{m_e}\right)^3\left(\frac{m_e}{m_\mu}\right)$$

PSAS'2024

Radiative−Recoil Diagrams at Order $\alpha^2(Z\alpha)^5$

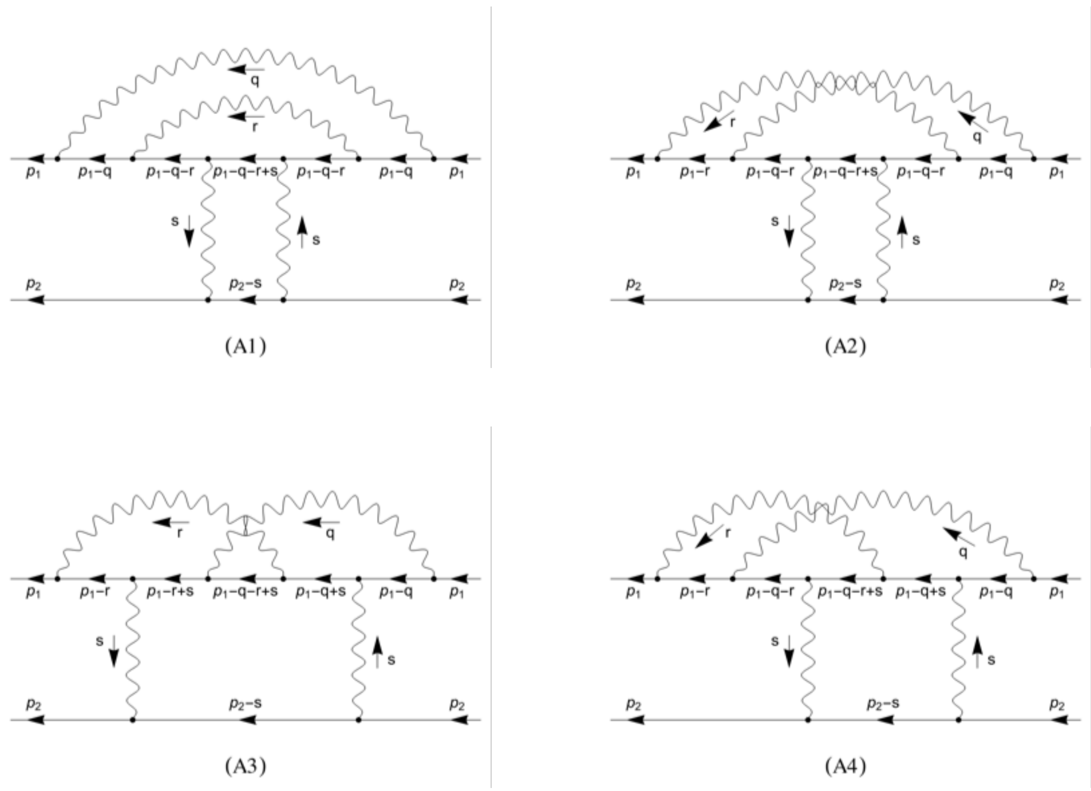

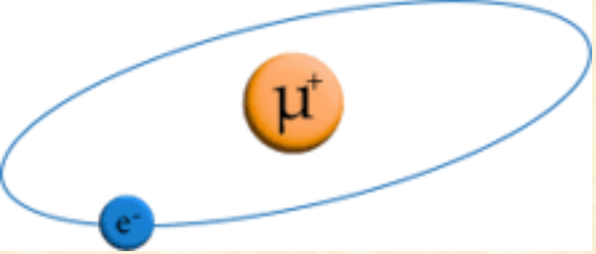

PSAS'2024

Radiative−Recoil Diagrams at Order $\alpha^2(Z\alpha)^5$

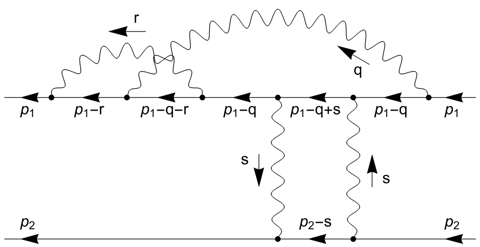

(B1)

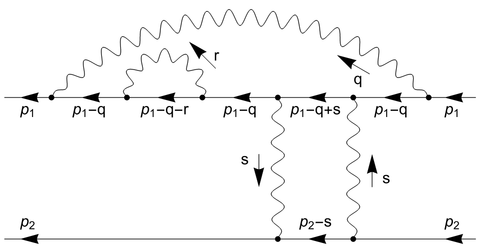

(B2)

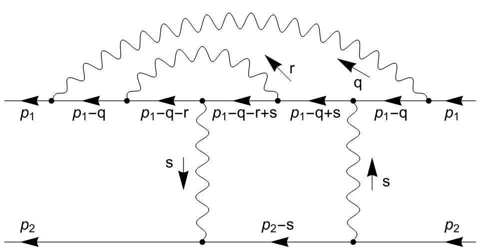

(B3)

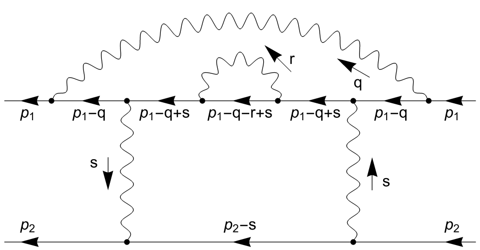

(B4)

PSAS'2024

Radiative–Recoil Diagrams at Order $\alpha^2(Z\alpha)^5$

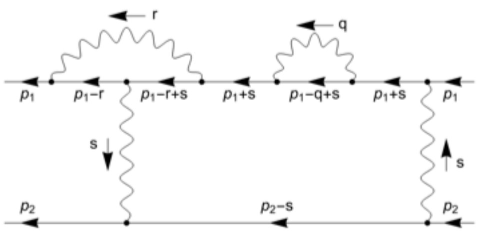

(C1)

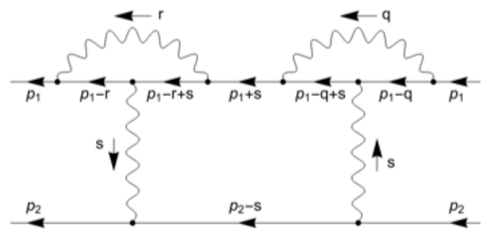

(C2)

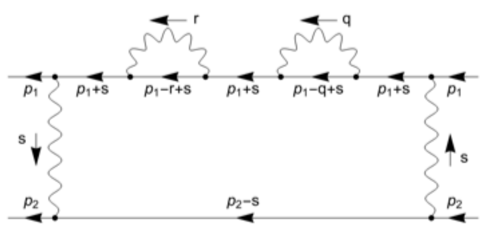

(C3)

PSAS'2024

Radiative−Recoil Diagrams at Order $\alpha^2(Z\alpha)^5$

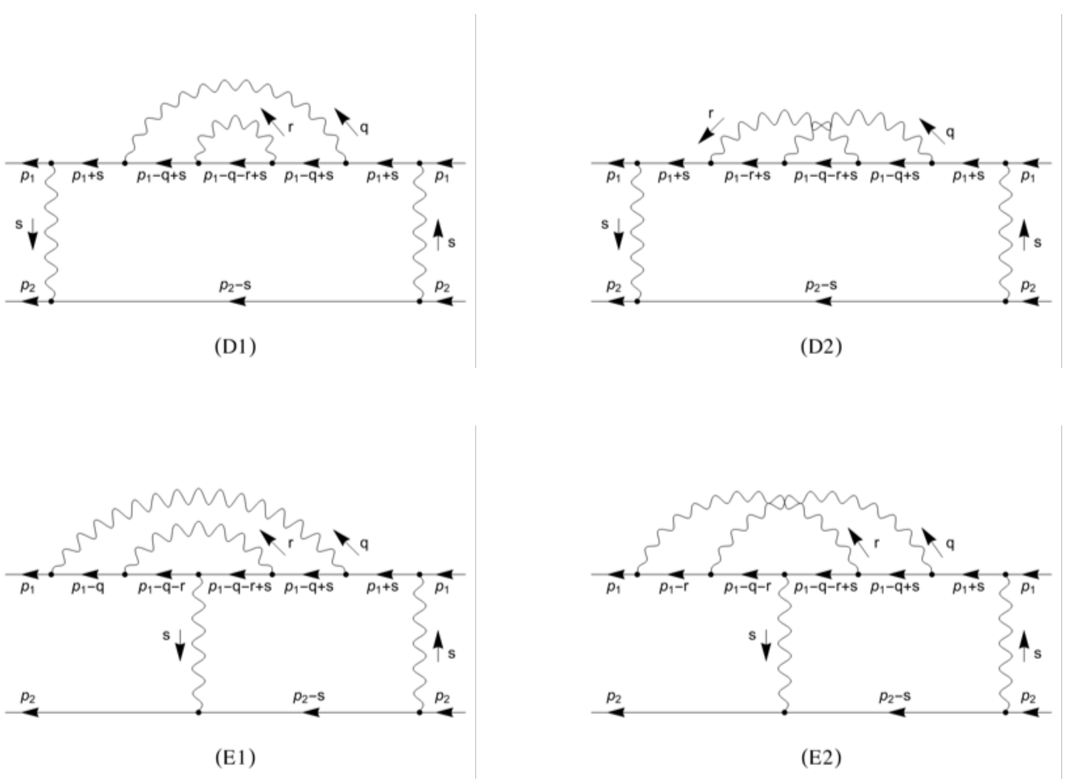

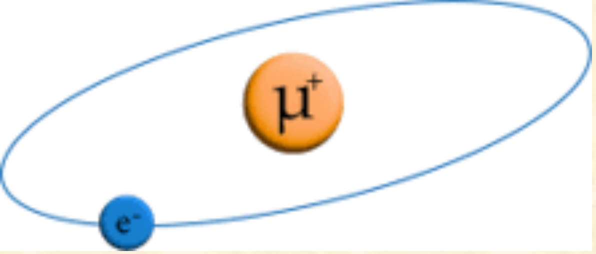

Radiative – Recoil Diagrams at Order $\alpha^2(Z\alpha)^5$

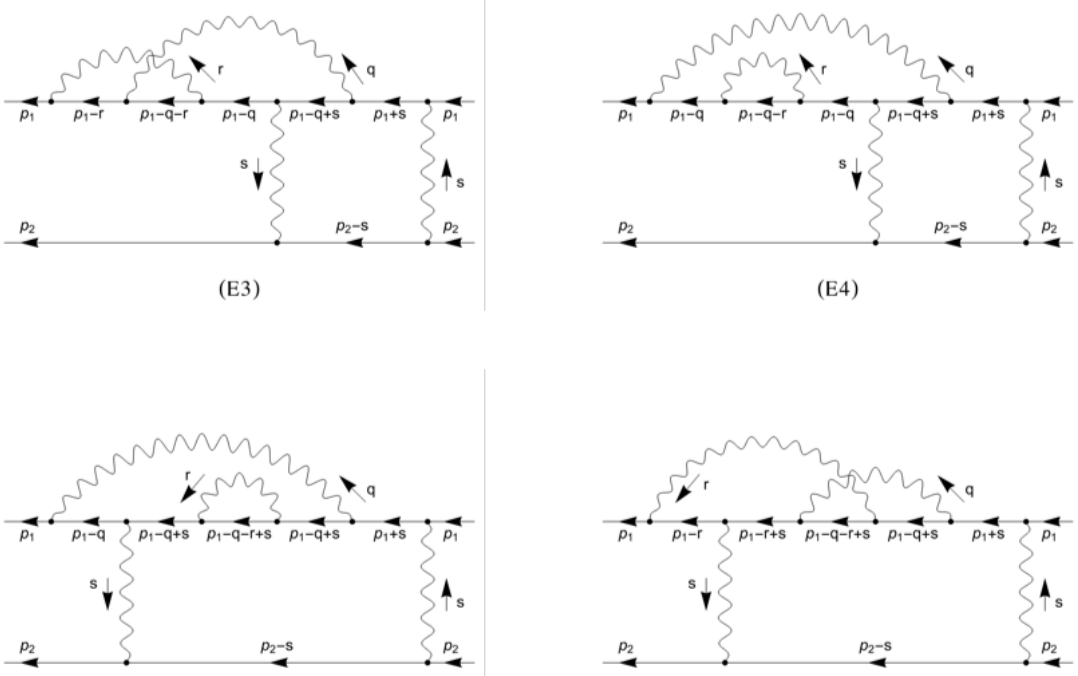

(E3) (E4)

(E5) (E6)

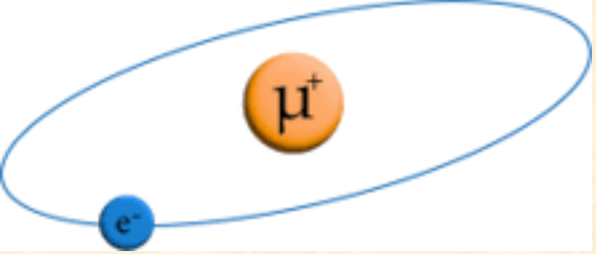

PSAS'2024

Next Steps: Recoil and Radiative-Recoil Corrections at order α^7

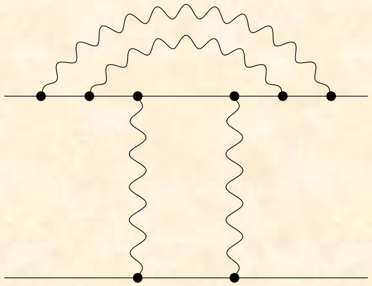

Radiative-recoil at order $\dfrac{m_e \alpha^2 (Z\alpha)^5}{n^3} \left(\dfrac{m_r}{m_e} \right)^3 \left(\dfrac{m_e}{m_\mu} \right)$

There are 19 diagrams with ladder photons, and two permutations of the photons (ladder and crossed) giving 2 x 19 = 38 diagrams when all diagrams with crossed photons are included. (Left-right symmetry has already been accounted for.) In all, there are 9155 separate three-loop Feynman integrals to compute.

The IBP relations have been used to express these 9155 integrals in terms of about 100 master integrals. The master integrals tend to be simpler than the ones they replace, but they are still non-trivial three-loop integrals.

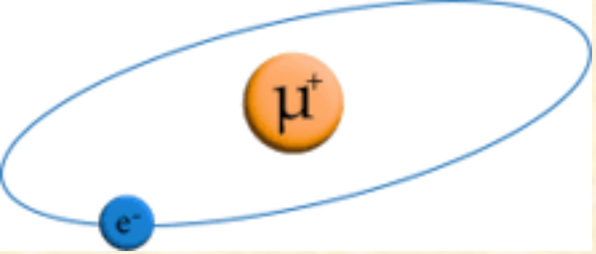

Integration by Parts Reduction

Integration by parts (IBP) identities are found using the fact that the integral of a divergence in d-dimensional space is zero.

$$0 = \int d^d q \, d^d s \, \frac{\partial}{\partial q^\mu} \left\{ \frac{v^\mu}{\text{dens}} \right\} = \int d^d q \, d^d s \, \frac{\partial}{\partial s^\mu} \left\{ \frac{v^\mu}{\text{dens}} \right\} \tag{.20}$$

where $v^\mu = q^\mu$, s^μ, or any external momentum vector. An example of the type of identity that is produced is

$$\begin{aligned} 0 &= \int d^d q \, d^d s \, \frac{\partial}{\partial q^\mu} \left\{ \frac{q^\mu}{(-q^2 + m_A^2)^\alpha (-(q-s)^2 + m_B^2)^\beta \cdots} \right\} \\ &= \int d^d q \, d^d s \left\{ \frac{d}{(\;)^\alpha (\;)^\beta \cdots} + \frac{2\alpha q^2}{(\;)^{\alpha+1} (\;)^\beta \cdots} + \frac{2\beta q \cdot (q-s)}{(\;)^\alpha (\;)^{\beta+1} \cdots} + \cdots \right\} \end{aligned} \tag{.21}$$

Many such identities are generated (using computer assistance) and are used to reduce a complicated integral containing very many terms to a linear combination of a few "master integrals". The relatively small set of master integrals are the only ones that must actually be evaluated.

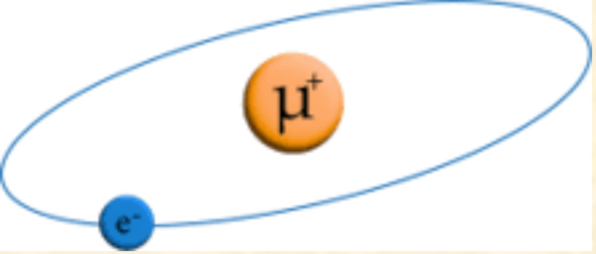

Example of One of the Master Integrals Needed for the Recoil Corrections

$$M(m_1, m_2) = \Phi^3 \int \frac{d^d q}{(2\pi)^d} \frac{d^d r}{(2\pi)^d} \frac{d^d s}{(2\pi)^d}$$
$$\times \frac{1}{(-(q-r)^2)(-q^2 + 2m_1 q \cdot n)(-s^2 - 2m_2 s \cdot n)(-(q+r-s)^2 + 2m_1(q+r-s) \cdot n)} .$$

First step, scale out one mass scale: $q = m_2 \tilde{q}$, $r = m_2 \tilde{r}$, $s = m_2 \tilde{s}$

Then $M(m_1, m_2) = m_2^{3d-8} J(x)$ where $x = \frac{m_1}{m_2}$ and

$$J(x) = \Phi^3 \int \frac{d^d \tilde{q}}{(2\pi)^d} \frac{d^d \tilde{r}}{(2\pi)^d} \frac{d^d \tilde{s}}{(2\pi)^d}$$
$$\times \frac{1}{(-(\tilde{q}-\tilde{r})^2)(-\tilde{q}^2 + 2x\tilde{q} \cdot n)(-\tilde{s}^2 - 2\tilde{s} \cdot n)(-(\tilde{q}+\tilde{r}-\tilde{s})^2 + 2x(\tilde{q}+\tilde{r}-\tilde{s}) \cdot n)} .$$

We use $d = 4 - 2\epsilon$. The factors $\Phi = -i(2\pi)^{2-\epsilon} e^{\epsilon \gamma_E}$ are included for convenience.

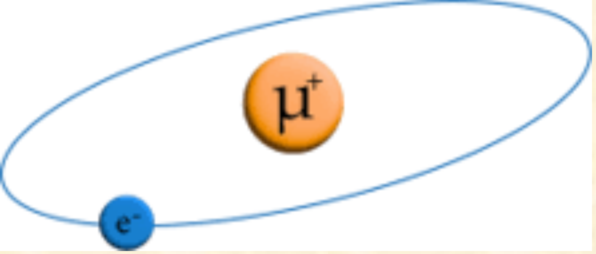

Method of Differential Equations

For illustration, consider the two-loop integral

$$J(x) = \Phi^2 \int \bar{d}^d q\, \bar{d}^d s \, \frac{1}{(-(q-s)^2)(-q^2 - 2xq\cdot n)(-s^2 + 2s\cdot n)}$$

In the "method of differential equations", the integral $J(x)$ must be calculated along with some companions. We set $J(x) \to J_2(x)$. (Also, $q \cdot n \to qn$, $s \cdot n \to sn$.)

We focus on the integrals $J_1(x)$, $J_2(x)$, and $J_3(x)$, where $J_1(x)$ and $J_3(x)$ are auxiliary integrals that has been included to make a set that is closed under differentiation.

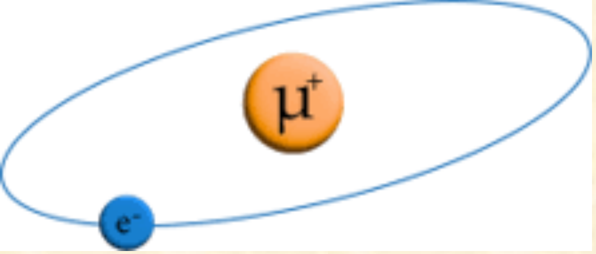

Method of Differential Equations

We focus on the integrals $J_1(x)$, $J_2(x)$, and $J_3(x)$, where $J_1(x)$ and $J_3(x)$ are auxiliary integrals that has been included to make a set that is closed under differentiation. We can get the value of $J_1(x)$ exactly. The $J_i(x)$ integrals are:

$$
\begin{aligned}
J_1(x) &\equiv \Phi^2 \int \bar{d}^d q \bar{d}^d s \, \frac{1}{(-q^2 - 2xqn)(-s^2 + 2sn)} \, , \\
J_2(x) &\equiv \Phi^2 \int \bar{d}^d q \bar{d}^d s \, \frac{1}{(-(q-s)^2)(-q^2 - 2xqn)(-s^2 + 2sn)} \, , \\
J_3(x) &\equiv \Phi^2 \int \bar{d}^d q \bar{d}^d s \, \frac{(-q^2)}{(-(q-s)^2)(-q^2 - 2xqn)(-s^2 + 2sn)} \, .
\end{aligned}
$$

$$
J_1(x) = x^{2(1-\epsilon)} e^{2\epsilon\gamma_E} \Gamma^2(-1+\epsilon)
$$

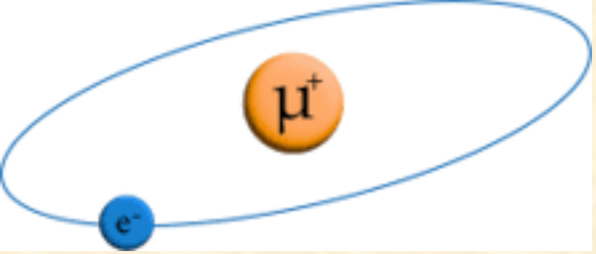

Method of Differential Equations

The x derivatives of the $J_i(x)$ integrals are easily found, and then the IBP identities were used to write the derivatives in terms of $J_i(x)$:

$$
\begin{aligned}
\frac{dJ_1(x)}{dx} &= \Phi^2 \int {\mathchar'26\mkern-12mu d}^d q\, {\mathchar'26\mkern-12mu d}^d s \, \frac{2qn}{(-q^2-2xqn)^2(-s^2+2sn)} \\
&= \frac{2(1-\epsilon)}{x} J_1(x)\,, \\
\frac{dJ_2(x)}{dx} &= \Phi^2 \int {\mathchar'26\mkern-12mu d}^d q\, {\mathchar'26\mkern-12mu d}^d s \, \frac{2qn}{(-(q-s)^2)(-q^2-2xqn)^2(-s^2+2sn)} \\
&= \frac{(1-\epsilon)}{x(1+x)(1+2x)} J_1(x) + \frac{3-4\epsilon-2\epsilon x-2x^2}{x(1+x)(1+2x)} J_2(x) + \frac{3(-1+\epsilon)}{x^2(1+2x)} J_3(x)\,, \\
\frac{dJ_3(x)}{dx} &= \Phi^2 \int {\mathchar'26\mkern-12mu d}^d q\, {\mathchar'26\mkern-12mu d}^d s \, \frac{(-q^2)(2qn)}{(-(q-s)^2)(-q^2-2xqn)^2(-s^2+2sn)} \\
&= \frac{4(-1+\epsilon)x}{(1+x)(1+2x)} J_1(x) + \frac{2(-5+6\epsilon)x}{(1+x)(1+2x)} J_2(x) + \frac{1+2(6-5\epsilon)x+8(1-\epsilon)x^2}{x(1+x)(1+2x)} J_3(x)\,.
\end{aligned}
$$

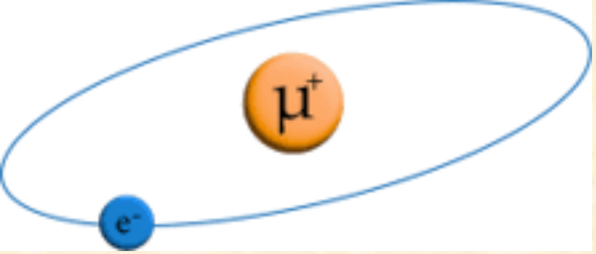

Method of Differential Equations

The set of coupled differential equations can be put in matrix form. This is a set of first order, ordinary, linear, homogeneous coupled differential equations. It is challenging to solve only because the coefficient matrix **A** depends on the independent variable x.

$$\frac{d}{dx}\vec{J} = \mathbf{A}\vec{J}$$

$$\vec{J} = \begin{pmatrix} J_1(x) \\ J_2(x) \\ J_3(x) \end{pmatrix} \quad , \quad \mathbf{A} = \begin{pmatrix} \frac{2(1-\epsilon)}{x} & 0 & 0 \\ \frac{(1-\epsilon)}{x(1+x)(1+2x)} & \frac{3-4\epsilon-2\epsilon x-2x^2}{x(1+x)(1+2x)} & \frac{3(-1+\epsilon)}{x^2(1+2x)} \\ \frac{4(-1+\epsilon)x}{(1+x)(1+2x)} & \frac{2(-5+6\epsilon)x}{(1+x)(1+2x)} & \frac{1+2(6-5\epsilon)x+8(1-\epsilon)x^2}{x(1+x)(1+2x)} \end{pmatrix}$$

Method of Differential Equations

As they stand, the differential equations for $J_1(x)$, $J_2(x)$ and $J_3(x)$ are challenging to solve. The trick is to make a change in dependent variable. The original differential equations are

$$\frac{d}{dx}\vec{J} = \mathbf{A}\vec{J}$$

then with the change of variable

$$\vec{J} = T\vec{I}$$

the differential equation becomes $\frac{d}{dx}\vec{I} = M\vec{I}$ with the new coefficient matrix M in "epsilon form":

$$M = T^{-1}AT - T^{-1}\frac{dT}{dx} = \epsilon \times (\text{function of } x \text{ only})$$

For that case at hand, we find

$$\frac{d}{dx}\vec{I} = \epsilon\left(\frac{a}{x} + \frac{b}{1+x}\right)\vec{I},$$

$$a = \begin{pmatrix} -2 & 0 & 0 \\ \frac{1413693}{146300} & -\frac{31857}{110} & \frac{32841}{220} \\ \frac{1393481}{73150} & -\frac{91427}{165} & \frac{31417}{110} \end{pmatrix} \quad , \quad b = \begin{pmatrix} 0 & 0 & 0 \\ -\frac{32643}{4180} & \frac{1877}{22} & -\frac{1989}{44} \\ -\frac{227509}{14630} & \frac{5311}{33} & -\frac{1877}{22} \end{pmatrix}$$

Method of Differential Equations

We assume the existence of a perturbative solution

$$\vec{I} = \vec{I}^{(0)} + \epsilon \vec{I}^{(1)} + \epsilon^2 \vec{I}^{(2)} + \cdots$$

where the $I^{(n)}$ are ϵ-independent function of x, and plug into the differential equation:

$$\frac{d}{dx}\left\{\vec{I}^{(0)} + \epsilon \vec{I}^{(1)} + \epsilon^2 \vec{I}^{(2)} + \cdots\right\} = \epsilon \left(\frac{a}{x} + \frac{b}{1+x}\right)\left\{\vec{I}^{(0)} + \epsilon \vec{I}^{(1)} + \epsilon^2 \vec{I}^{(2)} + \cdots\right\}$$

By considering the various orders individually, we find

$$\begin{aligned}
\frac{d}{dx}\vec{I}^{(0)} &= 0\,, \\
\frac{d}{dx}\vec{I}^{(1)} &= \left(\frac{a}{x} + \frac{b}{1+x}\right) I^{(0)}\,, \\
\frac{d}{dx}\vec{I}^{(2)} &= \left(\frac{a}{x} + \frac{b}{1+x}\right) I^{(1)}\,, \\
\frac{d}{dx}\vec{I}^{(3)} &= \left(\frac{a}{x} + \frac{b}{1+x}\right) I^{(2)}\,, \\
&\cdots
\end{aligned}$$

Method of Differential Equations

At $O(\epsilon^0)$ one has

$$\frac{d}{dx}\vec{I}^{(0)} = 0$$

so that

$$\vec{I}^{(0)} = \vec{h}^{(0)} = \left(h_1^{(0)}, h_2^{(0)}, h_3^{(0)}\right)^{\mathrm{T}}, \text{ a constant vector}$$

Method of Differential Equations

At $O(\epsilon^0)$ one has

$$\frac{d}{dx}\vec{I}^{(0)} = 0$$

so that

$$\vec{I}^{(0)} = \vec{h}^{(0)} = \left(h_1^{(0)}, h_2^{(0)}, h_3^{(0)}\right)^{\mathrm{T}}, \text{ a constant vector}$$

At $O(\epsilon^1)$ one has

$$\frac{d}{dx}\vec{I}^{(1)} = \left\{ \frac{1}{x}\, a.\vec{I}^{(0)} + \frac{1}{1+x}\, b.\vec{I}^{(0)} \right\}$$

so that

$$\begin{aligned} \vec{I}^{(1)} &= \int dx \left\{ \frac{1}{x} a.\vec{I}^{(0)} + \frac{1}{1+x} b.\vec{I}^{(0)} \right\} \\ &= \mathrm{HPL}(0;x)\, a.\vec{h}^{(0)} + \mathrm{HPL}(-1;x)\, b.\vec{h}^{(0)} + \vec{h}^{(1)} \end{aligned}$$

Method of Differential Equations

The "harmonic polylogarithm" functions $\mathrm{HPL}(a;x)$ are defined as a set of iterated integrals, starting with

$$\mathrm{HPL}(1;x) \equiv \int_0^x \frac{dt}{1-t} = -\ln(1-x) \quad , \quad \mathrm{HPL}(0;x) \equiv \ln x \quad , \quad \mathrm{HPL}(-1;x) \equiv \int_0^x \frac{dt}{1+t} = \ln(1+x)$$

and in general

$$\mathrm{HPL}(0,\cdots 0;x) \equiv \frac{1}{n!}\ln^n x \quad \text{for the HPL with first argument consisting of n zeros}$$

and

$$\mathrm{HPL}(a,a_1,\cdots,a_k;x) = \int_0^x dt\, f_a(t)\, \mathrm{HPL}(a_1,\cdots,a_k;t)$$

with

$$f_1(x) = \frac{1}{1-x} \quad , \quad f_0(x) = \frac{1}{x} \quad , \quad f_{-1}(x) = \frac{1}{1+x}$$

E. Remiddi and J. A. M. Vermaseran, Int. J. Mod. Phys. A **15**, 725 (2000)
T. Gehrmann and E. Remiddi, Comp. Phys. Commun. **141**, 296 (2001)
D. Maître, Comp. Phys. Commun. **174**, 222 (2006)

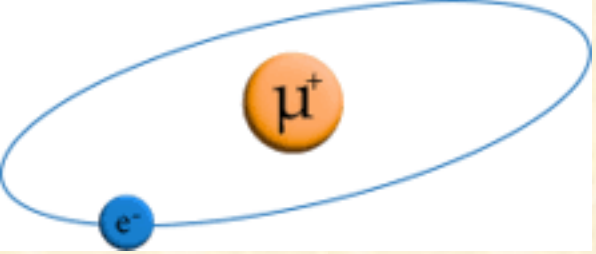

Method of Differential Equations

At $O(\epsilon^2)$ one has

$$\frac{d}{dx}\vec{I}^{(2)} = \left\{ \frac{1}{x}\, a.\vec{I}^{(1)} + \frac{1}{1+x}\, b.\vec{I}^{(1)} \right\}$$

so that

$$\begin{aligned}
\vec{I}^{(2)} &= \int dx \left\{ \frac{1}{x} a.\vec{I}^{(1)} + \frac{1}{1+x} b.\vec{I}^{(1)} \right\} \\
&= \mathrm{HPL}(0,0;x)\, a.a.\vec{h}^{(0)} + \mathrm{HPL}(0,-1;x)\, a.b.\vec{h}^{(0)} \\
&+ \mathrm{HPL}(-1,0;x)\, b.a.\vec{h}^{(0)} + \mathrm{HPL}(-1,-1;x)\, b.b.\vec{h}^{(0)} \\
&+ \mathrm{HPL}(0;x)\, a.\vec{h}^{(1)} + \mathrm{HPL}(-1,x)\, b.\vec{h}^{(1)} \\
&+ \vec{h}^{(2)}
\end{aligned}$$

Method of Differential Equations

At $O(\epsilon^3)$ one has

$$\frac{d}{dx}\vec{I}^{(3)} = \left\{ \frac{1}{x}\, a.\vec{I}^{(2)} + \frac{1}{1+x}\, b.\vec{I}^{(2)} \right\}$$

so that

$$\begin{aligned}
\vec{I}^{(3)} &= \int dx \left\{ \frac{1}{x} a.\vec{I}^{(2)} + \frac{1}{1+x} b.\vec{I}^{(2)} \right\} \\
&= \mathrm{HPL}(0,0,0;x)\, a.a.a.\vec{h}^{(0)} + 2^3 \text{ terms total involving } \vec{h}^{(0)} \\
&+ \mathrm{HPL}(0,0;x)\, a.a.\vec{h}^{(1)} + 2^2 \text{ terms total involving } \vec{h}^{(1)} \\
&+ \mathrm{HPL}(0;x)\, a.\vec{h}^{(2)} + \mathrm{HPL}(-1,x)\, b.\vec{h}^{(2)} \\
&+ \vec{h}^{(3)}
\end{aligned}$$

So finally $\vec{I} = \vec{I}^{(0)} + \epsilon \vec{I}^{(1)} + \epsilon^2 \vec{I}^{(2)} + \epsilon^3 \vec{I}^{(3)} + \cdots$

Method of Differential Equations

The integration constants are found by computing the expansion of the integrals about the point x=0 using "expansion by regions". The integrals are much simpler when x=0 that for non-zero values of x.

$$J_2(x) = \Phi^2 \int \bar{d}^d q \bar{d}^d s \, \frac{1}{(-(q-s)^2)(-s^2+2sn)(-q^2-2xqn)}.$$

In Region 1, $q \sim 1$, $s \sim 1$, so the expansion looks like

$$\begin{aligned} J_{21}(x) &= \Phi^2 \int \bar{d}^d q \bar{d}^d s \, \frac{1}{(-(q-s)^2)(-s^2+2sn)(-q^2)\left(1 - x\left(\frac{2qn}{-q^2}\right)\right)} \\ &= \Phi^2 \int \bar{d}^d q \bar{d}^d s \, \frac{1 + x\left(\frac{2qn}{-q^2}\right) + x^2\left(\frac{2qn}{-q^2}\right)^2 + x^3\left(\frac{2qn}{-q^2}\right)^3 + O(x^4)}{(-(q-s)^2)(-s^2+2sn)(-q^2)} \\ &= J_{210} + xJ_{211} + x^2 J_{212} + x^3 J_{213} + O(x^4). \end{aligned}$$

There are also contribution from regions where $q \sim x$, $s \sim 1$ and $q \sim x$, $s \sim x$.

These results have the form of a series expansion in x but are exact in the number of dimensions d. Comparison with the solution of the differential equation allows us to find the constants of integration.

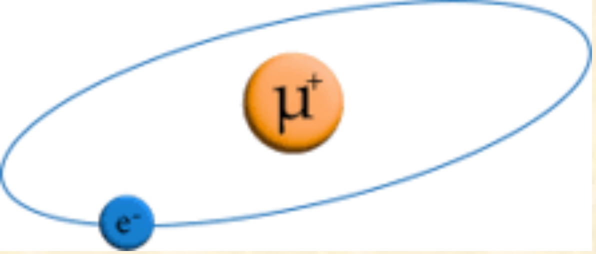

Conclusion

The calculation of recoil and radiative-recoil corrections to muonium and positronium energy levels at order α^7 (and exact in the particle masses) is in progress and should reduce the (QED) uncertainties in the muonium energies to a level comparable with expected experimental precisions.

Modern techniques for the evaluation of Feynman integrals is essential for this work, including the use of Integration by Parts (FIRE) for the reduction of many Feynman integrals to a (relatively) small set of ”master integrals”, and the use of the “method of differential equations”, along with “expansion by regions”, for the evaluation of the master integrals.

Thank you!

Greg Adkins
Franklin & Marshall College